International School of Atomic and Molecular Spectroscopy
12th Course: Ultrafast Dynamics of Quantum Systems:
Physical Processes and Spectroscopic Techniques
Erice, 15 - 30 June, 1997
Director: B. Di Bartolo

DIELECTRIC DESCRIPTION OF SEMICONDUCTORS:

FROM MAXWELL– TO SEMICONDUCTOR BLOCH–EQUATIONS

Ralph v. Baltz

Institut für Theorie der Kondensierten Materie
Universität Karlsruhe
D–76128 Karlsruhe, Germany

ABSTRACT

A tutorial on the dielectric description of matter is presented with particular attention to semiconductor optics. The first part focuses on general concepts like the construction of macroscopic fields, linear and quadratic response, and simple models how to describe the reaction of matter with respect to the electromagnetic field. Beginning with the two–level approximation of an atom, the second part will lead us to the semiconductor Bloch equations which are the today's standard model of semiconductor optics in the short time regime. Together with the Maxwell equations these form a closed set of dynamical equations for the electromagnetic field, polarization, and electron/hole population of a semiconductor upon optical excitations. Some selected applications and problems are added.

I. INTRODUCTION

For the electrodynamic description of semiconductors near the band edge, matter equations (or constitutive equations) are needed, which relate the charge density and current (or polarization) to the electromagnetic field. The simplest models to describe this coupling are the Lorentz-oscillator and the Drude-free carrier models. For a realistic description, however, the valence - conduction band continuum, excitonic effects, and electron/hole population dynamics must be considered. These phenomena are consistently described by the semiconductor Bloch equations which are a set of nonlinear, coupled differential-integral equations.
The scope of this article is twofold. First, in Chapter II, a survey on the macroscopic electromagnetic description of matter is presented, including some new aspects, discussion of basic models, and fundamentals of linear and nonlinear response.
Second, Chapter III is devoted to the foundation of the microscopic description of the light-matter interaction based on a two-level approach. This will guide us to the

Semiconductor Bloch Equations.
To round-off the material, some selected applications and supplements are given in Chapter IV. In particular some properties of the photogalvanic effect are discussed which describes a steady state unidirectional charge transport. Its spectacular properties are the absense of a "driving force" (in the sense of traditional irreversible thermodynamics) and the occurence of photovoltages up to 100 kV in ferroelectrics. Problems (with solutions) are added.

II. MACROSCOPIC ELECTRODYNAMICS

The electromagnetic field (EMF, or just "field") is descibed by the electrical and magnetic fields $\mathcal{E}(\mathbf{r},t), \mathcal{B}(\mathbf{r},t)$ which are coupled to matter through the charge– and current–density fields $\rho(\mathbf{r},t)$ and $\mathbf{j}(\mathbf{r},t)$. To formulate a closed set of equations one needs, besides the Maxwell–equations, either an explicit functional or a set of (differential–) equations for $\rho, \mathbf{j}$ in terms of $\mathcal{E}, \mathcal{B}$[1].
The standard book in the field of macroscopic electrodymamics is Landau and Lifshitz Vol. 8 [1], Wooten [2] gives an excellent introduction to optical properties of solids, and Klingshirn [3] provides a modern introduction to and an overview of semiconductor optics. Linear and nonlinear interactions of electromagnetic waves and matter is covered by several articles of this course [5] and the previous one [4].

II.A. Field Equations

The state of the microscopic electromagnetic field in matter is described by $\mathcal{E}_{\rm m}, \mathcal{B}_{\rm m}$ which satisfy the Maxwell–equations:

$$\epsilon_0\mu_0 \frac{\partial \mathcal{E}_{\rm m}(\mathbf{r},t)}{\partial t} - \text{curl}\, \mathcal{B}_{\rm m}(\mathbf{r},t) = -\mu_0\, \mathbf{j}_{\rm m}(\mathbf{r},t), \tag{1}$$

$$\frac{\partial \mathcal{B}_{\rm m}(\mathbf{r},t)}{\partial t} + \text{curl}\, \mathcal{E}_{\rm m}(\mathbf{r},\text{t}) = 0, \tag{2}$$

$$\epsilon_0\, \text{div}\, \mathcal{E}_{\rm m}(\mathbf{r},t) = \rho_{\rm m}(\mathbf{r},t), \tag{3}$$

$$\text{div}\, \mathcal{B}_{\rm m}(\mathbf{r},t) = 0. \tag{4}$$

The first set of Eqs. (1,2) which contain the time–derivatives of the fields are dynamical equations like the Newton–equations for a mechanical system, $\mathbf{j}_{\rm m}(\mathbf{r},t)$ plays the role of a "driving force". The two other Eqs. (3,4) are of different type and represent "rigid" conditions imposed by $\rho_{\rm m}(\mathbf{r},t)$ at time t. Together with the Lorentz–force (–density)

$$\mathbf{f}(\mathbf{r},t) = \rho(\mathbf{r},t)\mathcal{E}(\mathbf{r},t) + \mathbf{j}(\mathbf{r},t) \times \mathcal{B}(\mathbf{r},t) \tag{5}$$

these equations define the interacting field–matter system.
$\mathcal{E}_{\rm m}(\mathbf{r},t), \mathcal{B}_{\rm m}(\mathbf{r},t)$ contain large, spatially fluctuating contributions on an atomic scale and it is impossible to calculate or measure these fields. (A typical value of such field fluctuations is the field of a nucleus within atomic distances which is of the order of $\mathcal{E}_{\rm m} \approx 10^9 V/cm$.) To get rid of these fluctuations in a macroscopic description averaging upon so–called physically infinitesimally, small volumes have been known since the Lorentz–era, as a cureable method. If these volumes contain a large number of atoms they can again be treated macroscopically. During the last decade, however, the russian school around Keldysh [6],[7], recognized that this approach is not satisfactory for several reasons, e.g.

[1] vectors and tensors are written in boldface, electric and magnetic fields in caligrafic style

- the wavelength may be considerably reduced by a high refractive index,
- gyrotropy is related to the field gradient on molecular distances,
- the motion of charges is related to the actual field at the position of the particles rather than to the average field.

Therefore, averaging of physically infinitesimally small volumes is abandoned and replaced by the standard method of statistical physics averaging over the Gibbs–ensemble of all possible states of the field and matter, $\mathcal{E} =< \mathcal{E}_{\rm m} >$, $\mathcal{B} =< \mathcal{B}_{\rm m} >$. Owing to the linearity of the Maxwell-equations, this is formally simple and yields equations of the same structure as Eqs. (1-4):

$$\epsilon_0\mu_0\frac{\partial\mathcal{E}(\mathbf{r},t)}{\partial t} - \text{curl}\ \mathcal{B}(\mathbf{r},t) = -\mu_0\left[\mathbf{j}(\mathbf{r},t) + \mathbf{j}_{\rm ext}(\mathbf{r},t)\right], \tag{6}$$

$$\frac{\partial\mathcal{B}(\mathbf{r},t)}{\partial t} + \text{curl}\ \mathcal{E}(\mathbf{r},t) = 0, \tag{7}$$

$$\epsilon_0\text{div}\ \mathcal{E}(\mathbf{r},t) = \rho(\mathbf{r},t) + \rho_{\rm ext}(\mathbf{r},t), \tag{8}$$

$$\text{div}\ \mathcal{B}(\mathbf{r},t) = 0. \tag{9}$$

For convenience, the external sources $\rho_{\rm ext}(\mathbf{r},t), \mathbf{j}_{\rm ext}(\mathbf{r},t)$ have been separated from the matter fields $\rho(\mathbf{r},t) =< \rho_{\rm m}(\mathbf{r},t) >$, $\mathbf{j}(\mathbf{r},t) =< \mathbf{j}_m(\mathbf{r},t) >$. Here the adjective "external" refers to the control, not to the location of the charges, i.e. we assume that they are not affected by the charges in the medium.

II.B. Matter Equations

In a classical microscopic description the matter fields $\mathbf{j}_{\rm m}(\mathbf{r},t), \rho_{\rm m}(\mathbf{r},t)$ are defined by

$$\rho_{\rm m}(\mathbf{r},t) = \sum_{k=1}^{N} e_k\delta(\mathbf{r}-\mathbf{r}_k(t)), \quad \mathbf{j}_{\rm m}(\mathbf{r},t) = \sum_{k=1}^{N} e_k\mathbf{v}_k\delta(\mathbf{r}-\mathbf{r}_k(t)), \tag{10}$$

where the trajectories $r_i(t)$ of the particles with masses M_k and charges e_k are determined by the Newton-equations:

$$M_k\frac{d^2\mathbf{r}_k(t)}{dt^2} = e_k\mathcal{E}'_{\rm m}(\mathbf{r}_k,t) + e_k\mathbf{v}_k\times\mathcal{B}'_{\rm m}(\mathbf{r}_k,t), \quad \text{k=1...N.} \tag{11}$$

$\mathcal{E}'_{\rm m}, \mathcal{B}'_{\rm m}$ denote the fields without the self-contribution of particle $\#k$. For example, such calculations are presently performed numerically for high–power gyrotrons or particle accelerators by using a "particle in cell code".
For our purposes, a classical description of the EMF is sufficient, however, the matter must be treated quantum mechanically. In this case one has to find the wave–function (or statistical operator) from which the expectation values of the charge– and current–denstiy operators can be calculated. This will be done in Chapter III.
Instead of solving the microscopic equations within some approximation and performing the average afterwards, a much better strategy is to derive and solve manageable equations for $\rho(\mathbf{r},t), \mathbf{j}(\mathbf{r},t)$ in terms $\mathcal{E}(\mathbf{r},t)$, $\mathcal{B}(\mathbf{r},t)$. This is the main issue of this article.
A trivial example is the equation of continuity which likewise holds for the microscopic and macroscopic charge- and current–density

$$\frac{\partial\rho(\mathbf{r},t)}{\partial t} + \text{div}\ \mathbf{j}(\mathbf{r},t) = 0. \tag{12}$$

For stationary fields $\mathcal{E}(\mathbf{r})$ and $\mathcal{B}(\mathbf{r})$ are independent, whereas for time-dependent fields $\mathcal{B}(\mathbf{r},t)$ is fixed by $\mathcal{E}(\mathbf{r},t)$ up to a time-independent field (which will be left–out below). The same holds for $\rho(\mathbf{r},t)$ and $\mathbf{j}(\mathbf{r},t)$:

$$\mathcal{B}(\mathbf{r},t) = -\int_{t_0}^{t} \operatorname{curl}\mathcal{E}(\mathbf{r},t')\,dt', \tag{13}$$

$$\rho(\mathbf{r},t) = -\int_{t_0}^{t} \operatorname{div}\mathbf{j}(\mathbf{r},t')\,dt'. \tag{14}$$

Thus, there is only a single independent matter field, namely $\mathbf{j}(\mathbf{r},t) = \mathbf{j}[\mathcal{E}(\mathbf{r},t)]$ which can be written as a functional solely of $\mathcal{E}(\mathbf{r},t)$.
Instead of using the current density $\mathbf{j}(\mathbf{r},t)$ it is sometimes convenient to work with the polarization $\mathcal{P}(\mathbf{r},t)$ defined by

$$\mathbf{j}(\mathbf{r},t) = \frac{\partial\mathcal{P}(\mathbf{r},t)}{\partial t}, \qquad \rho(\mathbf{r},t) = -\operatorname{div}\mathcal{P}(\mathbf{r},t). \tag{15}$$

This definition includes the continuity equation (12).
Contributions from "free" charges or "magnetic" effects are not simply neglected but they are contained in $\mathcal{P}(\mathbf{r},t)$. Splitting the matter–current into free, bound, and magnitization currents is only useful for quasistationary fields but is neither necessary nor advantageous in solid state optics. At high frequencies the oscillation amplitude of "free" and "bound" charges are of the same order, hence, there is no physical difference. For an experimental investigation of "magnetic" contributions in the IR range see Grosse [8]. The price to pay leaving the magnetization $\mathcal{M}(\mathbf{r},t)$ out of the game is the need of a space–dependent polarization field even when in the convential description $\mathcal{P}$ and $\mathcal{M}$ are (piecewise) constant. But this can be done on equal footing with spatial dispersion (see chapter II.C.).
In the following, we shall preferably work with $\mathbf{j}(\mathbf{r},t)$ to describe "metallic" systems ("free" charges, intraband dynamics) and $\mathcal{P}(\mathbf{r},t)$ for "dielectric" behaviour ("bound" charges, interband dynamics). This is motivated by the fact that for slowly varying fields (with respect to time and space) the following relations hold

$$\mathbf{j}(\mathbf{r},t) = \sigma\mathcal{E}(\mathbf{r},t), \qquad \mathcal{P}(\mathbf{r},t) = \epsilon_0\chi\mathcal{E}(\mathbf{r},t), \tag{16}$$

where constants σ, χ represent the electrical conductivity and susceptibility. These are the simplest form of matter–equations. Systems which contain both types of carriers are conventionally modelled just by adding both contributions.
On a phenomenological level the functional relation between $\mathbf{j}(\mathbf{r},t)$, $\mathcal{P}(\mathbf{r},t)$ and $\mathcal{E}(\mathbf{r},t)$ may be represented by a power-expansion in terms of the field

$$\mathbf{j}(\mathbf{r},t) = \sum_{k=1}^{\infty}\mathbf{j}^{(k)}(\mathbf{r},t), \qquad \mathcal{P}(\mathbf{r},t) = \sum_{k=1}^{\infty}\mathcal{P}^{(k)}(\mathbf{r},t), \qquad \mathbf{j}^{(k)},\ \mathcal{P}^{(k)} \propto \mathcal{E}^k. \tag{17}$$

Expansion (17) is possible if $\mathcal{E}$ is much smaller than typical atomic fields $\mathcal{E}_{at} \approx 10^9$ V/cm. Although such fields cannot be produced in steady state laboratory experiments, ten times larger fields have been recently created in short laser pulses. In addition, fields may be strongly enhanced near resonances as, e.g. in the dynamical Stark–effect.

Within a classical description the dynamics of conduction electrons in a semiconductor or a metal is governed by a hydrodynamic type of equation which is the generalization of the famous Drude–model:

$$\left(\frac{\partial}{\partial t} + \gamma\right)\mathbf{j}(\mathbf{r},t) + \beta\,\operatorname{grad}\rho(\mathbf{r},t) = \frac{-e}{m^*}\,\rho(\mathbf{r},t)\mathcal{E}(\mathbf{r},t). \tag{18}$$

m^* is the effective mass, e the charge, γ the relaxation rate of the carriers, and β denotes a dispersion constant which is proportional to the diffusion constant. (For metals $\beta = 3v_F^2/5$, where v_F is the Fermi–velocity.) In addition to the standard Drude model, Eq.(18) includes diffusion. (The coupling to the magnetic field via the Lorentz–force is left–out for simplicity.) For applications to metal–optics near the plasma–edge see Forstmann and Gerhards [9], for plasmons see e.g. v. Baltz [10].
Bound charges like optical phonons can be modelled by an oscillator type of equation which is known as the Lorentz–model [3]:

$$\left(\frac{\partial^2}{\partial t^2} + \gamma\frac{\partial}{\partial t} + \omega_0^2 + \beta\Delta\right)\mathcal{P}(\mathbf{r},t) = \epsilon_0\Omega_p^2\mathcal{E}(\mathbf{r},t), \tag{19}$$

where ω_0 is oscillation frequency, n_0 is the density of oscillators, $\Omega_p^2 = n_0e^2/m^*\epsilon_0$, and $\beta\Delta\mathcal{P}$ accounts for the coupling to neighbouring oscillators [11].
These differential equations are supplemented by boundary conditions like the continuity of the normal component of $\mathbf{j}$ or $\mathcal{D} = \epsilon_0\mathcal{E} + \mathcal{P}$ at surfaces or interfaces. Note, $\mathcal{E}(\mathbf{r},t)$ denotes the total electrical field in matter - rather than the external field.

Problems:
1.) Find the general solutions of Eqs.(18-19) for the homogeneous case. (Neglect nonlinearity in Eq.(18) replacing $\rho(\mathbf{r},t)$ by $-|e|n_0$, where n_0 is the equilibrium electron density.) Use $\mathbf{j}(-\infty) = 0$ and $\mathcal{P}(-\infty) = 0$ as boundary conditions.

2.) Screening of a point–charge by free carriers.
Find the stationary solution for the induced charge–density and potential of a point charge in a metal within the hydrodynamic model as given by Eq. (18). Compare with the bare Coulomb–potential.

II.C. Linear Response

The general form of the linear part of expansion (17) between the current or polarization and the field reads:

$$\mathbf{j}_\alpha^{(1)}(\mathbf{r},t) = \int\int \sigma_{\alpha\beta}^{(1)}(\mathbf{r},\mathbf{r}',t-t')\mathcal{E}_\beta(\mathbf{r}',t')d^3\mathbf{r}'dt', \tag{20}$$

$$\mathcal{P}_\alpha^{(1)}(\mathbf{r},t) = \epsilon_0\int\int \chi_{\alpha\beta}^{(1)}(\mathbf{r},\mathbf{r}',t-t')\mathcal{E}_\beta(\mathbf{r}',t')d^3\mathbf{r}'dt'. \tag{21}$$

For brevity we shall discuss only the $\mathcal{P}$–$\mathcal{E}$ relation (21) in the following, as the current–field relation (20) is analogous.
The "susceptibility–kernel" χ takes into account that the coupling between field and polarization generally is

- nonlocal, i.e. the field at $\mathbf{r}'$ can cause a polarization at another point $\mathbf{r}$,
- has a memory, i.e. $\mathcal{P}$ may exist for some time after the field is switched–off,
- $\mathcal{P}$ may not be parallel to $\mathcal{E}$, i.e. χ is a second rank tensor where α,β denote cartesian components. Summation over repeated indices is implied.

For homogeneous matter susceptibility tensor $\chi_{\alpha,\beta}$ is solely a function of $\mathbf{r}-\mathbf{r}'$ so that the integral relation (21) becomes a convolution:

$$F(t) := [f_1 \otimes f_2](t) = \int_{-\infty}^{\infty} f_1(t-t')f_2(t')dt' \tag{22}$$

which simplifies to a product under Fourier–transformation

$$F(\omega) = f_1(\omega) \cdot f_2(\omega). \tag{23}$$

$f(t)$, $f(\omega)$ denote a Fourier–pair:

$$f(t) = \int_{-\infty}^{\infty} f(\omega) e^{-i\omega t} \frac{d\omega}{2\pi}, \quad f(\omega) = \int_{-\infty}^{\infty} f(t) e^{+i\omega t} dt. \tag{24}$$

The $(\mathbf{r}, t)$–Fourier–transformation is used in the following "plane–wave" form:

$$\chi^{(1)}_{\alpha\beta}(\mathbf{r}, t) = \int\int e^{i(\mathbf{qr}-\omega t)} \chi^{(1)}_{\alpha\beta}(\mathbf{q}, \omega) \frac{d^3\mathbf{q} d\omega}{(2\pi)^4}, \tag{25}$$

$$\chi^{(1)}_{\alpha\beta}(\mathbf{q}, \omega) = \int\int e^{-i(\mathbf{qr}-\omega t)} \chi^{(1)}_{\alpha\beta}(\mathbf{r}, t) d^3\mathbf{r} dt, \tag{26}$$

$$\mathcal{P}^{(1)}_{\alpha}(\mathbf{q}, \omega) = \epsilon_0 \chi^{(1)}_{\alpha\beta}(\mathbf{q}, \omega) \mathcal{E}_{\beta}(\mathbf{q}, \omega). \tag{27}$$

The $\mathbf{q}, \omega$ dependence of the susceptibility (or σ) is termed spatial and temporal dispersion, respectively. $\chi(\mathbf{q}, \omega) = \frac{i}{\epsilon_0 \omega} \sigma(\mathbf{q}, \omega)$.
To keep the presentation simple we omit the tensorial structure of χ, the superscript (1), and spatial dispersion. The most important property of $\chi(t - t')$ is the property of causality: There is no response before the perturbation is turned on. This is one of the fundamental laws of nature.

$$\chi(t - t') \equiv 0, \quad t' > t. \tag{28}$$

Some consequences of causality in the frequency domain will be exploited in the next section.
In contrast to the real response kernel $\chi(t-t')$ in the time–domain its Fourier–transform $\chi(\omega)$ is complex

$$\chi(\omega) = \chi_1(\omega) + i\chi_2(\omega) = \int_{-\infty}^{\infty} \chi(t'') e^{i\omega t''} dt''. \tag{29}$$

The real and imaginary parts of $\chi(\omega)$ are even and odd functions of frequency. (This holds regardless of causality.) Moreover, the real part of $\sigma(\omega)$ and the imaginary part of $\chi(\omega)$ are related to dissipation, whereas the other parts are connected to dispersion. For details see [1], [2] or e.g. an overview given by Di Bartolo in this book [12].
As an illustration of the time and frequency dependence of response functions we state the results for the Drude– and Lorentz–models (omitting spatial dispersion, $\mathbf{q} = 0$. See problems 1,3, and 4), Figs. 1,2.
The Drude conductivity and susceptibility are:

$$\sigma(t - t') = \frac{n_0 e^2}{m^*} e^{-\gamma(t-t')} \theta(t - t'), \tag{30}$$

$$\sigma(\omega) = \frac{n_0 e^2}{m^*} \frac{1}{\gamma - i\omega}, \tag{31}$$

$$\chi(t - t') = \frac{\omega_p^2}{\gamma} \left[1 - e^{-\gamma(t-t')}\right] \theta(t - t'), \tag{32}$$

$$\chi(\omega) = -\frac{\omega_p^2}{\omega(\omega + i\gamma)}, \quad \omega_p^2 = \frac{n_0 e^2}{m^* \epsilon_0}, \tag{33}$$

where n_0 and ω_p denote the density and plasma–frequency, respectively.

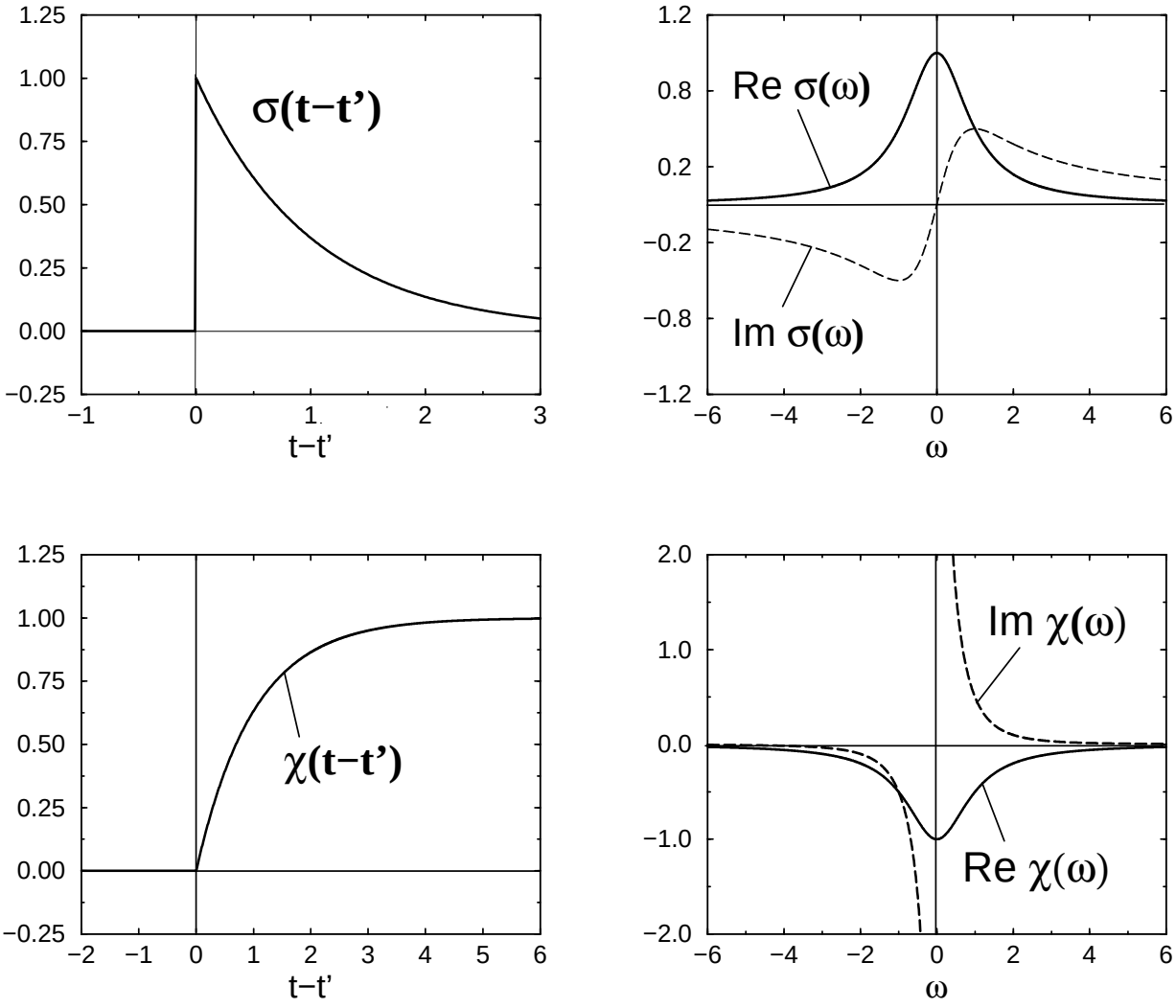

Fig. 1 *Drude–conductivity and susceptibility. (Left) Time domain, (right) frequency domain. (Dimensionless units).*

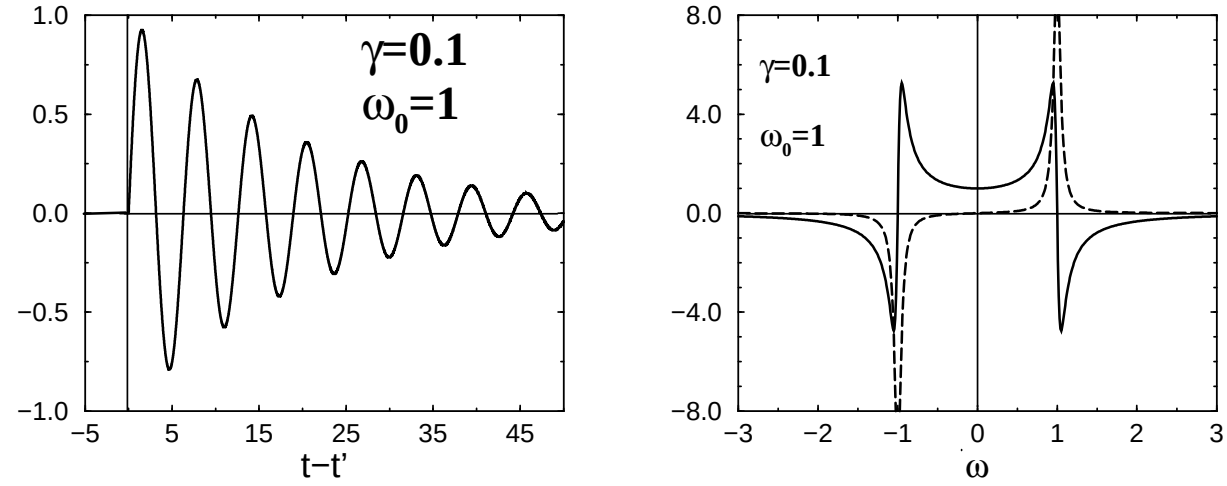

Fig. 2 *Lorentz–susceptibility. (Left) Time domain, (right) frequency domain. (Dimensionless units).*

The Lorentz–susceptibility is given by:

$$\chi(t-t') = \frac{\Omega_p^2}{\Omega_0}\, e^{-\frac{\gamma}{2}(t-t')}\, \sin\left[\Omega_0(t-t')\right]\, \theta(t-t'), \tag{34}$$

$$\chi(\omega) = \frac{\Omega_p^2}{\omega_0^2-\omega^2-i\omega\gamma}, \quad \Omega_0^2=\omega_0^2-(\frac{\gamma}{2})^2. \tag{35}$$

It is convenient to decompose all vector-fields into longitudinal and transverse components with respect to wave vector $\mathbf{q}$, i.e.

$$\mathcal{E}(\mathbf{q},\omega)=\mathcal{E}_\ell(\mathbf{q},\omega)+\mathcal{E}_t(\mathbf{q},\omega)=(\mathcal{E}\cdot\mathbf{n_q})\,\mathbf{n_q}+\mathbf{n_q}\times(\mathcal{E}\times\mathbf{n_q})\,, \tag{36}$$

with unit vector $\mathbf{n_q}=\mathbf{q}/|\mathbf{q}|$. Even for homogeneous and isotropic systems, like Jellium, the reaction of the charged particles with respect to transverse and longitudinal fields is different, i. e. $\sigma(\mathbf{q},\omega)$ and $\chi(\mathbf{q},\omega)$ are tensors with two different principal components:

$$\mathbf{j}(\mathbf{q},\omega)=\epsilon_0\,\hat{\sigma}(\mathbf{q},\omega)\,\mathcal{E}(\mathbf{q},\omega)=\sigma_\ell(\mathbf{q},\omega)\mathcal{E}_\ell(\mathbf{q},\omega)+\sigma_t(\mathbf{q},\omega)\mathcal{E}_t(\mathbf{q},\omega). \tag{37}$$

Transverse fields, $\mathbf{j}\cdot\mathbf{q}=0$, are source–free, div $\mathbf{j}=0$, and, thus, do not create charge fluctuations: $\rho=0$. On the other hand, longitudinal fields, $\mathbf{j}\parallel\mathbf{q}$, are irrotational and create charge fluctuations: $\rho(\mathbf{q},\omega)=q\,j(\mathbf{q},\omega)/\omega$.

Problems:

3.) Calculate $\sigma(\mathbf{q},\omega)$ and $\epsilon(\mathbf{q},\omega)=1+i\sigma(\mathbf{q},\omega)/\omega\epsilon_0$ for longitudinal and transverse fields in a metal by Fourier–transformation of Eq. (18). $\epsilon(\mathbf{q},\omega)=0$ gives the dispersion of longitudinal collective excitations(=plasmons) [10].

4.) Calculate the transverse electrical susceptibility for bound charges by Fourier–transformation of Eq.(19). The poles of $\chi(\mathbf{q},\omega)$ (or $\epsilon=1+\chi$) gives the dispersion of transverse excitations. Compare with transverse optical phonons [3].

II.D. Nonlinear Response

In intense laser pulses many nonlinear phenomena are observed which are described by the second and higher order terms in the expansion (17). For an introduction and survey see, e.g., Boyd [13].
For simplicity we consider only the second–order current–field relation and omit spatial dispersion. Then, an expansion analogous to Eq.(20) holds:

$$\mathbf{j}^{(2)}_\alpha(\mathbf{r},t)=\int\int\sigma^{(2)}_{\alpha\beta\gamma}(t-t',t-t'')\mathcal{E}_\beta(\mathbf{r},t')\mathcal{E}_\gamma(\mathbf{r},t'')dt'dt''. \tag{38}$$

As in the linear case, causality restricts the time–integration to $t',t''<t$. In Fourier–space the double time–integral is reduced to a single, convolution–type integral:

$$\mathbf{j}^{(2)}_\alpha(\mathbf{r},\omega) = \int\sigma^{(2)}_{\alpha\beta\gamma}(\omega',\omega-\omega')\mathcal{E}_\beta(\mathbf{r},\omega')\mathcal{E}_\gamma(\mathbf{r},\omega-\omega')\frac{d\omega'}{2\pi}, \tag{39}$$

$$\sigma^{(2)}_{\alpha\beta\gamma}(\omega_1,\omega_2) = \int\int\sigma^{(2)}_{\alpha\beta\gamma}(t_1,t_2)e^{i(\omega_1t_1+\omega_2t_2)}dt_1dt_2. \tag{40}$$

The quadratic response is described by a third rank tensor which, in contrast to linear response, exists only in noncentrosymmetric crystals like $GaAs$ or $LiNbO_3$. Germanium

and Silicon, on the other hand, have a center of inversion and the first nonvanishing nonlinear contribution begins in terms of a cubic fourth rank tensor $\sigma^{(3)}_{\alpha\beta\gamma\delta}$.

As ω_1, ω_2 are dummy variables in Eq.(38), $\chi^{(2)}_{\alpha,\beta\gamma}(\omega_1, \omega_2)$ is symmetric (or can be chosen to be symmetric) with respect to the pair of indices (α, ω_1), (β, ω_2). Further symmetry properties can be found, e.g. in [13].

As an example, we consider the case in which the optical field incident upon a nonlinear optical medium characterized by a quadratic conductivity $\sigma^{(2)}$ consists of two distinct frequency components ω_1, ω_2, $(\omega_2 > \omega_1)$:

$$\mathcal{E}(t) = \mathcal{E}_1 e^{-i\omega_1 t} + \mathcal{E}_2 e^{-i\omega_2 t} + \big[1 \to -1, 2 \to -2\big], \tag{41}$$

$$\mathcal{E}(\omega) = 2\pi\big[\mathcal{E}_1\delta(\omega - \omega_1) + \mathcal{E}_2\delta(\omega - \omega_2)\big] + \big[1 \to -1, 2 \to -2\big]. \tag{42}$$

$[1 \to -1]$ means a change of ω_1 by $-\omega_1$ in the preceding expression etc. and $\mathcal{E}_{-1} = \mathcal{E}_1^*$. Then, according to Eq.(38) the second–order current contribution is given by [2]

$$\begin{aligned}
\mathbf{j}^{(2)}(\omega) = 2\pi\Big\{ & \\
& + \mathcal{E}_1^2\sigma^{(2)}(+\omega_1, +\omega_1)\,\delta(\omega - 2\omega_1) + \mathcal{E}_2^2\sigma^{(2)}(+\omega_2, +\omega_2)\,\delta(\omega - 2\omega_2) && (43)\\
& + 2\mathcal{E}_1\mathcal{E}_2\sigma^{(2)}(+\omega_1, +\omega_2)\,\delta(\omega - [\omega_1 + \omega_2]) && (44)\\
& + 2\mathcal{E}_1^*\mathcal{E}_2\sigma^{(2)}(-\omega_1, +\omega_2)\,\delta(\omega - [\omega_2 - \omega_1]) && (45)\\
& + \big[1 \to -1, 2 \to -2\big], & \\
& + 2\left[|\,\mathcal{E}_1\,|^2\,\sigma^{(2)}(-\omega_1, +\omega_1) + |\,\mathcal{E}_2\,|^2\,\sigma^{(2)}(-\omega_2, +\omega_2)\right]\delta(\omega)\Big\}. && (46)
\end{aligned}$$

Via the Maxwell–equations the induced current will in turn be the source of radiation. The various terms describe:

- second harmonic generation (SHG), Eq. (43)
- sum frequency generation (SFG), Eq. (44)
- difference frequency generation (DFG), Eq. (45)
- optical rectification (OR), photogalvalvanic effect (PGE), Eq. (46).

For the description of high–frequency current phenomena SHG, SFG, and DFG the point of view of a "free" charge current $\mathbf{j}(\mathbf{r}, t)$ and a "bound" charge current $\frac{\partial}{\partial t}\mathcal{P}(\mathbf{r}, t)$ are fully equivalent. However, this is different for the $\omega = 0$ component of the current and the polarization. The $\omega = 0$ component of $\mathcal{P}(\mathbf{r}, t)$, known as optical rectification describes an isothermal and isobaric change of the value of the polarization only. It does not give rise to a steady–state current or an electromotive force. In contrast to OR which describes charge separation across a finite distance, the $\omega = 0$ component of $\mathbf{j}(\mathbf{r}, t)$ may be considered as a charge separation across infinite distances. In addition, OR is nondissipative and can occur in the nominally transparent part of the spectrum (where Im $\chi(\omega) = 0$) whereas absorption of light and, hence, dissipation is needed to induce a direct (nonsupra)–current. For instationary excitations OR leads to a transient current whose shape is given by the time derivative of the intensity profile $j \propto \dot{I}(t)$, whereas, the PGE would lead to a current pulse which follows $I(t)$. (As OR is of minor importance in nonlinear optics little attention is usually paid for this subtle distinction and the notation OR is sometimes ambiguous.) The occurence of a direct current upon light

[2] In nonlinear optics a redundant notation with three frequency arguments is used : $\sigma^{(2)}(\omega_3, \omega_2, \omega_1)$. This is technically unnecessary in that ω_3 is always $\omega_1 + \omega_2$. Analogous for the higher order terms.

absorption in nonlinear crystals is now called photogalvanic effect (or bulk photovoltaic effect) and some of its exciting properties will be discussed in chapter IV.C.
As in linear response there are Kramers–Kronig relations for second and higher order. However, nonlinear phenomena are almost exclusively studied in the nonabsorptive part of the spectrum so that these relations are of no practical importance.

III. QUANTUM THEORY OF ATOMS AND SEMICONDUCTORS

Our macroscopic description of linear and nonlinear properties of matter has mostly made use of a power series of the current or polarization in terms of the field. Under resonant excitation this approximation fails to provide an adequate description of the response and a description by (nonlinear) equations like Eq.(99) are more appropriate. Under resonant conditions it is usually sufficient to deal only with the two levels which are nearly resonantly excited by the light. Even for semiconductors the optical transitions between valence and conduction band can be visualized as transitions between a collection of two–level systems (TLS).
The discussion of the Semiconductor–Bloch–equations (SBE) will proceed in three steps. First we study the dynamics of atoms near resonance in the two–level approximation and derive the atomic Bloch equations for the polarization. Next, this result is generalized to the case of a semiconductor with noninteracting valence and conduction bands. Eventually, the influence of Coulomb–interaction between the electron–hole excitations is considered. This will lead us to the SBE which presently are the standard model of semiconductor optics in particular to describe nonlinear short pulse phenomena. Presumably Stahl [11] was the first to use such equations in a systematic way to describe the electrodynamics of semiconductors near the band edge.
According to the scope of this article the presentation is kept on an introductory level and "sophisticated" techniques are avoided. A thorough derivation of the SBE is outlined by Haug and Koch [14], which is the standard book in this field, or by Zimmermann [15].

III.A. Dynamics of the Two–Level–System

The optical properies of TLS are presented in many texts, my favorites are the Feynman lectures Vol. 3 in connection with the Ammonia maser [16] and the book by Allen and Eberly [17].
To describe the optical properties of an atom near resonance, we only retain the pair of nearly resonant stationary states $|1>$ and $|2>$ with energies ϵ_1 and ϵ_2, $(\epsilon_2 > \epsilon_1)$, respectively. In particular, we assume that these states have s and p symmetry so that the optical transition is dipole–allowed. In this restricted "base" the state vector of the atom

$$| \psi(t) >= c_1(t)|1> + c_2(t)|2> \tag{47}$$

is represented by the coefficients c_1, c_2 which can be arranged in form of a two–component column vector $\mathbf{c}$. $\mathbf{c}^\dagger = (c_1, c_2)$.
The time–dependence of $c_j(t)$ is governed by the Schrödinger equation:

$$i\hbar \frac{\partial}{\partial t} \begin{pmatrix} c_1 \\ c_2 \end{pmatrix} = \hat{\mathbf{H}} \begin{pmatrix} c_1 \\ c_2 \end{pmatrix}. \tag{48}$$

The first term in the Hamiltonian

$$\hat{\mathbf{H}} = \hat{\mathbf{H}}_\mathbf{0} - \hat{\mathbf{P}}\mathcal{E}(t), \qquad \hat{\mathbf{H}}_\mathbf{0} = \begin{pmatrix} \epsilon_1 & 0 \\ 0 & \epsilon_2 \end{pmatrix}, \qquad \hat{\mathbf{P}} = \begin{pmatrix} 0 & p \\ p^* & 0 \end{pmatrix}. \tag{49}$$

describes the isolated atom, whereas the second term is the interaction with the electrical field of the classical light wave in electrical dipole approximation. p is the dipole matrix–element between $|1>$ and $|2>$.
From the Schrödinger–equation (48) we obtain two coupled first–order differential equations for $c_1(t)$ and $c_2(t)$:

$$\begin{aligned} i\hbar\dot{c}_1(t) &= \epsilon_1 c_1(t) - p\mathcal{E}(t)c_2(t), & (50)\\ i\hbar\dot{c}_2(t) &= \epsilon_2 c_2(t) - p^*\mathcal{E}(t)c_1(t). & (51) \end{aligned}$$

From $c_1(t), c_2(t)$ the energy and the dipole moment of the TLS are fixed by:

$$\begin{aligned} E(t) &= \mathbf{c}^\dagger\hat{\mathbf{H}}_0\mathbf{c} = \epsilon_1|c_1(t)|^2 + \epsilon_2|c_2(t)|^2 = \frac{\epsilon_1+\epsilon_2}{2} + \frac{\epsilon_2-\epsilon_1}{2}I(t), & (52)\\ p(t) &= \mathbf{c}^\dagger\hat{\mathbf{P}}\mathbf{c} = pP(t) + p^*P^*(t), & (53)\\ I(t) &= |c_2(t)|^2 - |c_1(t)|^2, & (54)\\ P(t) &= c_1^*(t)c_2(t), & (55) \end{aligned}$$

where $I(t)$ is the inversion and $P(t)$, the complex dipole moment, which are the basic quantities to describe the physics of the TLS.
For the unperturbed atom ($\mathcal{E} \equiv 0$) the time evolution of $c_j(t)$ is

$$c_j(t) = d_j e^{-i\epsilon_j t/\hbar}, \quad j = 1, 2, \tag{56}$$

with constant prefactors d_1 and d_2. Hence, $I(t)$ =const and $P(t) = d_1^* d_2 \exp(-i\omega_0 t)$, where $\omega_0 = (\epsilon_2 - \epsilon_1)/\hbar$ is the transition frequency between the energy levels ϵ_j.
To solve the coupled system of differential Eqs.(50,51) we first split–off the free time evolution:

$$\begin{aligned} c_j(t) &= d_j(t)e^{-i\epsilon_j t/\hbar}, \qquad j = 1, 2, & (57)\\ \dot{d}_1(t) &= i\frac{p}{\hbar}\mathcal{E}(t)e^{-i\omega_0 t}d_2(t), & (58)\\ \dot{d}_2(t) &= i\frac{p^*}{\hbar}\mathcal{E}(t)e^{+i\omega_0 t}d_1(t). & (59) \end{aligned}$$

These equations are somewhat simpler than Eqs.(50,51), but an analytical solution is still not accessible. Near resonance, however, the product of $\mathcal{E}(t) = \mathcal{E}_0\cos(\omega t)$ and $e^{\pm i\omega_o t}$ contains a term which is almost constant and another one which oscillates rapidly. This fast oscillating term will be neglected in the following (this is termed "rotating wave approximation", RWA. See the end of this chapter).
Besides the transition frequency ω_0, there are two other characteristic frequencies:

- $\nu = \omega - \omega_0$, which is called "detuning", and
- $\omega_R = p\mathcal{E}_0/\hbar$, the Rabi-frequency.

Within the RWA, the system of differential Eqs.(58,59):

$$\begin{aligned} \dot{d}_1(t) &= i\frac{\omega_R}{2}\, e^{+i\nu t}d_2(t), & (60)\\ \dot{d}_2(t) &= i\frac{\omega_R}{2}\, e^{-i\nu t}d_1(t), & (61) \end{aligned}$$

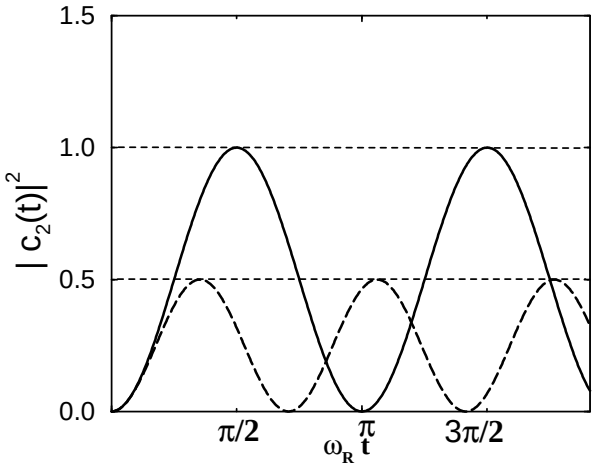

Fig. 3 *Rabi–oscillations of the excited state population. (Full line) Resonant excitation, (dashed line) detuned excitation, $\omega = 2\omega_0$.*

still contains an explicit time dependence. Nevertheless, Eqs.(60,61) transform to the harmonic oscillator when inserting Eq.(60) into Eq.(61). In contrast to the standard oscillator equation, it contains "imaginary" rather than real damping:

$$\left[\frac{d^2}{dt^2} + i\nu\frac{d}{dt} + (\frac{\omega_R}{2})^2\right] d_1(t) = 0. \tag{62}$$

The solution can be found by the standard exponential Ansatz and reads:

$$d_1(t) = \left[a\cos(\frac{\Omega_R}{2}t) + b\sin(\frac{\Omega_R}{2}t)\right]\exp\left(i\frac{\nu}{2}t\right), \tag{63}$$

$$d_2(t) = -i\frac{2}{\omega_R}e^{-i\nu t}\dot{d}_1(t). \tag{64}$$

$\Omega_R = \sqrt{\omega_R^2 + \nu^2}$ is the "detuned" Rabi–frequency.
For example, at resonance and for the initial conditions $c_1(0) = 1$, $c_2(0) = 0$ we have:

$$d_1(t) = \cos(\frac{\omega_R}{2}t), \quad d_2(t) = i\sin(\frac{\omega_R}{2}t). \tag{65}$$

The probability to find the atom in the excited state is given by the absolute square of $d_2(t)$ which oscillates with the Rabi–frequency ω_R. At time $t_1 = \pi/\omega_R$ the atom is in the excited state and at $2\pi/\omega_R$ it is back again in the ground state. For detuned fields, the oscillation period becomes shorter and the amplitude is less than unity, Fig. 3.
For example, for atomic sodium the parameters for the $3s - 3p$ transition are: $p = 2.5a_Be, \lambda_0 = 589nm$. For an intensity of 127 Watt cm^{-2} the Rabi–frequency $\omega_R/2\pi =$ 1GHz becomes larger than the natural line width [13].
Next, we reformulate the problem and set up an equation for the complex dipole moment and the inversion themselves in terms of the driving field. $\mathcal{P}(t)$ and $I(t)$ likewise fulfill first order differential equations

$$\left[\frac{d}{dt} + i\omega_0\right] P(t) = -i\frac{p^*}{\hbar}\mathcal{E}(t)I(t) + \dot{P}_{sc}, \tag{66}$$

$$\frac{dI(t)}{dt} = -4\,\mathrm{Im}\left[\frac{p}{\hbar}\mathcal{E}(t)\mathcal{P}^*(t)\right] + \dot{I}_{sc}. \tag{67}$$

The advantage of these equations with respect to Eqs.(50,51) is the possibility to include damping (=collisions, scattering, or incoherent motion). In a simple phenomenological description this is accomplished by:

$$\dot{P}_{sc} = -\frac{P}{T_2}, \quad \dot{I}_{sc} = -\frac{I(t) - I_{eq}}{T_1}. \tag{68}$$

T_1 and T_2 are called "longitudinal" and "transverse" relaxation times. As I is the square of an amplitude we expect $T_2 \approx 2T_1$. I_{eq} is the equilibrium value of the inversion in the absence of the driving field. At zero temperature $I_{eq} = -1$.
Without damping, there is a conserved quantity,

$$4\,|P(t)|^2 + I^2(t) = const \tag{69}$$

which may be used to eliminate the inversion from Eq.(66). Its origin becomes obvious from a remarkable analogy between a two-level system and a spin-system in a magnetic field: The level-splitting between the ground state and the excited state of the atom plays the role of a constant magnetic field in z-direction, whereas the light field is equivalent to an oscillatory magnetic field in x-direction. The expectation value of the spin operator, $\mathbf{S} = (S_1, S_2, S_3)$, is closely related to the complex dipole moment and the inversion:

$$\begin{aligned} S_1 &= <\hat{\sigma}_x> = c_1^* c_2 + c_1 c_2^* \quad = 2\ \mathrm{Re}\ P(t), & (70)\\ S_2 &= <\hat{\sigma}_y> = -ic_1^* c_2 + ic_1 c_2^* = 2\,\mathrm{Im}\ P(t), & (71)\\ S_3 &= <\hat{\sigma}_z> = \mid c_1 \mid^2 - \mid c_2 \mid^2 \ = -I(t), & (72) \end{aligned}$$

and obeys the atomic Bloch-equations:

$$\frac{d\mathbf{S}(t)}{dt} = \mathbf{\Omega} \times \mathbf{S}(t) + \dot{\mathbf{S}}_{sc}, \quad \dot{\mathbf{S}}_{sc} = \begin{pmatrix} -S_1/T_2 \\ -S_2/T_2 \\ -(S_3 - S_3^{eq})/T_1 \end{pmatrix}, \quad \mathbf{\Omega} = \begin{pmatrix} -\omega_R \cos\omega t \\ \omega_R \sin\omega t \\ -\omega_0 \end{pmatrix}, \tag{73}$$

which describe a rotation of $\mathbf{S}$ around vector $\mathbf{\Omega}$ at each instant of time. The second component of $\mathbf{\Omega}$ is a consequence of the RWA so that the notation eventually becomes obvious.
In the absence of relaxation, the length of the Bloch vector $\mathbf{S}$ is conserved and its motion can be nicely visualized, Figs. 4,5. We consider two limiting cases. Without a time dependent field, $\mathbf{S}$ rotates on a cone around the z-axis which is called Larmor-precession:

$$\mathbf{S}(t) = (a \sin\omega_0 t, a \cos\omega_0 t, \mathrm{const})\,. \tag{74}$$

If the system is excited at resonance from initial state $\mathbf{S}(0) = (0, 0, 1)$ it performes Rabi–oscillations:

$$\mathbf{S}(t) = (\sin\omega_R t \sin\omega_0 t, \sin\omega_R t \cos\omega_0 t, \cos\omega_R t)\,. \tag{75}$$

Problems:

5.) Calculate $d_j(t)$ according to Eqs.(63,64) for arbitrary detuning and initial conditions $d_1(0) = 1$ and $d_2(0) = 0$.

6.) At resonance there are states of the coupled TLS–electrical field with time–independent probabilities $|d_j(t)|^2 = \mathrm{const}$. Find these states!

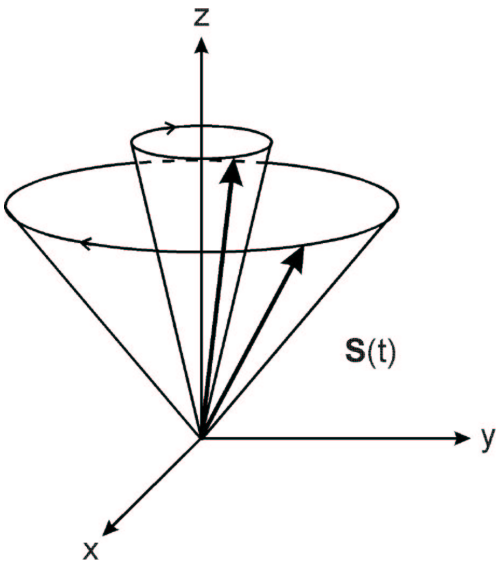

Fig. 4 *Larmor–precession of the Bloch–vector, according to Eq.(74).*

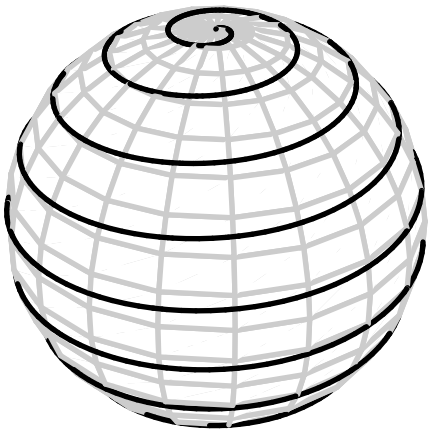

Fig. 5 *Rabi–oscillation: Trace of the Bloch–vector upon resonant excitation (without damping), according to Eq.(75),* $0 \leq \omega_R t \leq \pi$.

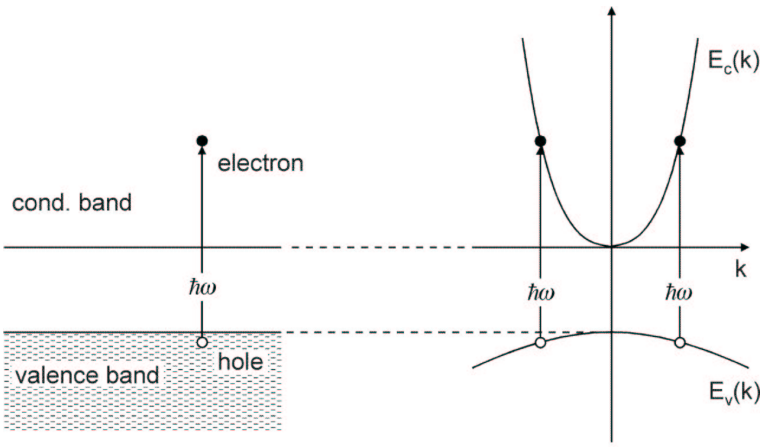

Fig. 6 *Sketch of the band structure and optical transitions in a semiconductor.*

III.B. Semiconductor with Noninteracting Bands

The generalization of the atomic Bloch-equations to the case of a two–band semiconductor is straightforward, Fig 6. In the dipole approximation the optical transitions are vertical in k-space. Without scattering or nonradiative recombination processes, the two band semiconductor is just an assembly of uncoupled TLS and resembles the case of a inhomogeneously broadened line problem in atomic physics:

$$i\hbar\frac{\partial P(\mathbf{k},t)}{\partial t} = \Big[E_c(k)-E_v(k)\Big]P(\mathbf{k},t)+p\mathcal{E}(t)\Big[n_c(\mathbf{k},t)-n_v(\mathbf{k},t)\Big]+i\hbar\dot{P}_{sc}, \quad (76)$$

$$\frac{\partial n_c(\mathbf{k},t)}{\partial t} = -2\,\mathrm{Im}\,\Big[p\mathcal{E}(t)P^*(\mathbf{k},t)\Big]+\dot{n}_c^{sc}, \quad (77)$$

$$\frac{\partial n_v(\mathbf{k},t)}{\partial t} = +2\,\mathrm{Im}\,\Big[p\mathcal{E}(t)P^*(\mathbf{k},t)\Big]+\dot{n}_v^{sc}. \quad (78)$$

Eqs.(76-78) are called optical Bloch equations. In the absence of scattering the equations are uncoupled and $\mathbf{k}$ merely acts as a parameter. From the complex polarization $P(\mathbf{k},t)$ the electronic polarization $\mathcal{P}(\mathbf{r},t)$ of the semiconductor can be obtained from

$$\mathcal{P}(t)=\frac{1}{V}\sum_{k,s}[p_{cv}(k)P(\mathbf{k},t)+cc], \quad (79)$$

where V denotes the crystal volume (normalization volume of the wave–functions) which eventually drops out when performing the sum over wave numbers $\mathbf{k}$ by an integral

$$\frac{1}{V}\sum_{k,s}\ldots = 2\frac{1}{(2\pi)^d}\int\ldots d^dk. \quad (80)$$

$d=1,2,3$ is the spatial dimension and the factor 2 arises from spin. The k-dependence of the dipole matrix element $p_{cv}(\mathbf{k})$ can often be neglected near the band edge.
As an application, we state the linear response result where $n_c=f_c(k)$ and $n_v=f_v(k)$ are the Fermi-functions. As k is merely a parameter, the required solution of Eq.(76) can be found by the Ansatz

$$P(k,t)=Q(k,t)\exp\Big[i(\epsilon_v(k)-\epsilon_c(k))-\hbar\omega)t\Big] \quad (81)$$

with a simple integration for $Q(k,t)$. When separating the different Fourier–components the susceptibility can be read–off:

$$\chi(\omega)=\frac{1}{V\epsilon_0}\sum_{k,s}|p_{cv}(k)|^2\left\{\frac{f_v(k)-f_c(k)}{E_c(k)-E_v(k)-\hbar(\omega+i\delta)}+\frac{f_v(k)-f_c(k)}{E_c(k)-E_v(k)+\hbar(\omega+i\delta)}\right\}. \quad (82)$$

For parabolic bands and $\mathbf{k}$–independent dipole matrix elements the absorptive part of the susceptibility becomes proportional to the joint density of states which rises as a square–root above the gap $\chi_2(\omega)\propto\sqrt{\hbar\omega-E_g}$.

III.C. Semiconductor Bloch-Equations

We are close to the summit of our tour towards the SBE – which is today's standard model of semiconductor optics. Two features have not yet been taken into account:

- There is a change in Coulomb energy of the interacting many electron ground state when exciting an electron to the conduction band and leaving a hole behind. This (exchange) interaction turns out to be an attractive Coulomb potential.

- With increasing band filling there is a renormalization of the electron/hole band energy by the (repulsive) electron/hole Coulomb interaction:

$$\begin{aligned} i\hbar\frac{\partial P(\mathbf{k},t)}{\partial t} &= \Big[E_g + E_e(k) + E_h(k)\Big]P(\mathbf{k},t) + \\ &\quad \Big[n_e(\mathbf{k},t) + n_h(\mathbf{k},t) - 1\Big]\hbar\Omega_R(\mathbf{k},t) + i\hbar\dot{P}_{sc}, \qquad (83) \\ \frac{\partial n_c(\mathbf{k},t)}{\partial t} &= -2\,\mathrm{Im}\left\{\Omega_R P^*(\mathbf{k},t)\right\} + \dot{n}_c^{sc}, \qquad (84) \\ \frac{\partial n_h(\mathbf{k},t)}{\partial t} &= -2\,\mathrm{Im}\left\{\Omega_R P^*(\mathbf{k},t)\right\} + \dot{n}_h^{sc}. \qquad (85) \end{aligned}$$

For convenience, the change in population of the valence band is formulated within the hole picture as indicated by the index h:

$$n_v(\mathbf{k},t) = 1 - n_h(\mathbf{k},t), \qquad E_v(\mathbf{k},t) = -E_g - E_h(\mathbf{k},t). \qquad (86)$$

$E_e(\mathbf{k},t)$, $E_h(\mathbf{k},t)$ are the electron/hole (Hartee–Fock) energies including the interaction with other electrons/holes. For parabolic bands these are:

$$E_j(\mathbf{k},t) = \frac{\hbar^2\mathbf{k}^2}{2m_j} - \frac{1}{V}\sum_q V(\mathbf{k}-\mathbf{q})n_j(\mathbf{q},t), \quad j = e,h. \qquad (87)$$

Note, $m_h > 0$. $\Omega_R(\mathbf{k},t)$ denotes the Rabi-frequency function:

$$\hbar\Omega_R(\mathbf{k},t) = p\mathcal{E}(t) + \frac{1}{V}\sum_q V(\mathbf{k}-\mathbf{q})P(\mathbf{q},t). \qquad (88)$$

$V(\mathbf{q})$ is the Fourier–transform of the electron–hole Coulomb–potential screened by a "background" dielectric constant $\bar{\epsilon}$:

$$V(\mathbf{q}) = \frac{e^2}{\epsilon_0\bar{\epsilon}q^2}, \qquad V(\mathbf{r}) = \frac{e^2}{4\pi\epsilon_0\bar{\epsilon}r}. \qquad (89)$$

In addition, this interaction will be screened by mobile electrons and holes in terms of a dielectric function $\epsilon_\ell(\mathbf{q},\omega)$ as discussed in problem 3.

IV. APPLICATIONS AND SUPPLEMENTS

IV.A. Causality and Kramers–Kronig Relations

There are three equivalent formulations of causality [18]:

1. The original formulation (28) of the polarization or current response just states, that the present value of the polarization does not depend on future fields:

$$\chi(t-t') \equiv 0, \; t' > t. \qquad (90)$$

   A function of this type is called a causal function.

2. The Fourier–transform (29) of a causal function

$$\chi(\omega_1 + i\omega_2) = \int_0^\infty \chi(t) e^{i\omega_1 t - \omega_2 t} dt \tag{91}$$

is an analytic function of $\omega = \omega_1 + i\omega_2$ in the upper part of the complex ω–plane, $\omega_2 > 0$. In this half–plane $\chi(\omega)$ has no poles or other singularities. For real ω, $\chi(\omega)$ is the boundary value of this analytic function.

3. Real and imaginary parts of $\chi(\omega)$ are connected by the Kramers–Kronig relations:

$$\chi_1(\omega) = \frac{+1}{\pi} P\!\!\!\!\!\!\int_{-\infty}^{\infty} \frac{\chi_2(\omega')}{\omega' - \omega} d\omega', \tag{92}$$

$$\chi_2(\omega) = \frac{-1}{\pi} P\!\!\!\!\!\!\int_{-\infty}^{\infty} \frac{\chi_1(\omega')}{\omega' - \omega} d\omega'. \tag{93}$$

Apart from causality the following assumptions have been made to derive Eqs.(92,93):

- $\chi(\omega)$ has no singularities on the real ω–axis,
- $\chi(\omega)$ tends to zero at large frequencies.

If there are singularities in $\chi(\omega)$ which lie perfectly on the real axis (like the pole of the Drude susceptibility at $\omega = 0$, Eq.(33)) these terms have to be subtracted before applying the Kramers–Kronig relations: $\chi \to \bar{\chi} = \chi(\omega) - \chi_{\text{pole}}(\omega)$.
If $\chi(\omega)$ tends to a finite value at $\omega = \infty$, $\chi \to \bar{\chi} = \chi(\omega) - \chi(\infty)$ in Eqs.(92,93). For the magnetic susceptibility such a constant term arises from the diamagnetic contribution. In addition, Im $\chi_{mag} > 0$ is not guaranteed! [20]. However, the electrical susceptibility and the conductivity always fulfill $\chi(\infty) = 0$, $\sigma(\infty) = 0$. To describe the low–frequency properties of semiconductors (e.g. the contribution of optical phonons) it is sometimes convenient to neglect dispersion at high frequencies (e.g. of the electronic interband transitions) by introducing a constant χ_∞. For instance, for $GaAs$, $\epsilon_\infty = 1 + \chi_\infty = 10.6$ which holds up to half of the band edge at $\hbar\omega = 1.4eV$ [3]. The resistivity, on the other hand, has a first order pole at $\omega = \infty$ so that this pole has to be likewise subtracted from $\rho(\omega)$ before applying the Kramers–Kronig relations to $\rho = 1/\sigma$.
In Eqs.(92,93) the "P" denotes "principal value" which is a prescription how to treat the singular integral:

$$g(\omega) = \frac{1}{\pi} P\!\!\!\!\!\!\int_{-\infty}^{\infty} \frac{f(\omega')}{\omega' - \omega} d\omega' = \lim_{\delta \to 0^+} \frac{1}{\pi} \left(\int_{-\infty}^{\omega - \delta} + \int_{\omega + \delta}^{\infty} \right) \frac{f(\omega')}{\omega' - \omega} d\omega'. \tag{94}$$

In mathematics this relation is termed Hilbert– transformation.
Another way to interpret this limiting process is to replace the singular function $\frac{1}{\omega' - \omega}$ by a "regularized" function $P\frac{1}{\omega' - \omega}$ which are almost identical except near the singularity. There $P\frac{1}{\omega - \omega'}$ becomes zero in an (anti–) symmetrical fashion. For instance, $\frac{1}{\omega' - \omega}$ is put to zero (anti–)symmetrically around the singularity from $\omega - \delta$ to $\omega + \delta$ with $\delta \to 0$. This is just a reformulation of Eq.(94). But any other symmetrical replacement is equivalent and resembles the way the Dirac delta–function is constructed, e.g.

$$P\frac{1}{\omega} \simeq \frac{\omega}{\omega^2 + \delta^2}, \quad \delta(\omega) \simeq \frac{1}{\pi} \frac{\delta}{\omega^2 + \delta^2}, \quad \delta \to 0^+. \tag{95}$$

$P\frac{1}{\omega}$ has a precise meaning only under an intergral and is - like $\delta(\omega)$ - another example of a distribution.

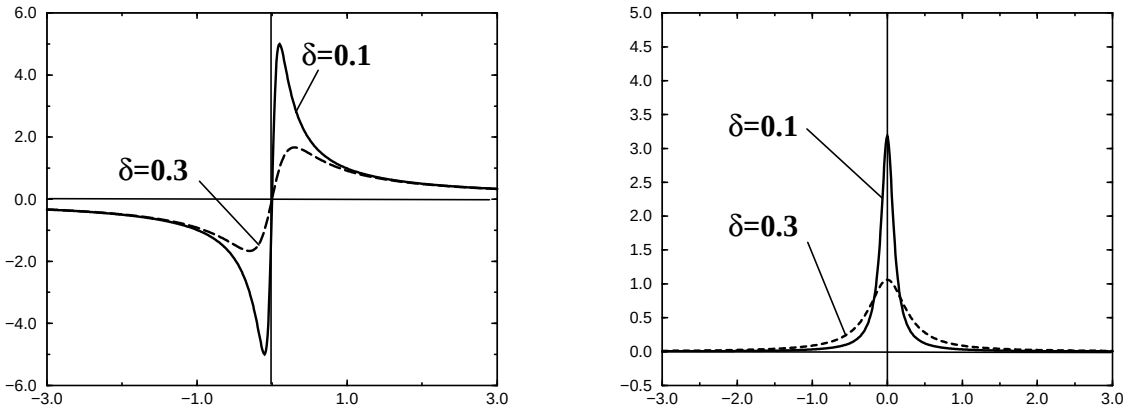

Fig. 7 *Sequence of function which "converge" to the principal value (left) and to the delta function (right).*

Because of the singular structure of the integrand in Eqs. (92-94) these integrals cannot be simply numerically calculated, e.g. by just using a Simpson–routine. For some elementary functions $f(\omega)$, however, the integral and the limiting process in Eq.(94) can be done analytically (see problem 8). In other cases, $f(\omega)$ is too complex or only known numerically. Then, one possibility to perform the Hilbert–transformation numerically is to fit $f(\omega)$ piecewise by a parabolic function (or a cubic spline), do the integral piecewise analytically and eventually sum all contributions numerically. Problem 9 supplies another possibility.
Traditionally, the proof of the Kramers–Kronig relations is by using tools from complex analysis, e.g. [1],[2], or [12]. A much shorter and almost "trivial" proof, however, can be found in Stößel's book on Fourier–Optik [19]:

- A causal function (90) trivially obeys $\chi(t) \equiv \chi(t)\theta(t)$, where $\theta(t)$ is the unit step function. This relation holds if there is no singular part in $\chi(t)$ of the type $\chi_\infty \delta(t)$ which corresponds to a nonvanishing contribution in $\chi(\omega)$ at $\omega = \infty$.

- Using the convolution theorem (22,23), Fourier–transformation yields:

$$\chi(\omega) = \chi(\omega) \otimes \theta(\omega). \tag{96}$$

  As $\theta(t)$ does not converge to zero at $t = \infty$ its Fourier–transform needs, as usual in such cases, an adiabatic switching–off factor $exp(-\delta t)$ to define the integral

$$\theta(\omega) = \int_0^\infty 1 \cdot e^{i\omega t} e^{-\delta t}\, dt = \frac{1}{\delta - i\omega} = P\frac{i}{\omega} + \pi\delta(\omega). \tag{97}$$

- Separation of real and imaginary parts in Eq.(96) immediately leads to the Kramers–Kronig relations (92,93).

For a detailed discussion of Kramers–Kronig relations in connection with sum–rules we refer to the seminal article by Martin [20].

Problems:

7.) Sketch the loci of the singularities of $\chi(\omega)$ and $\sigma(\omega)$ in the complex ω–plane.
(a) For the Drude and (b) the Lorentz–model. (Use results of problems 3,4).

8.) Calculate the Hilbert–transform (94) of the "box–function" box(ω) = 1 for $\mid \omega \mid < 1$, otherwise box(ω) = 0.

9.) The Hilbert–transformation (94) is again a convolution and, thus, may be transformed to a product in time–domain

$$g(t) = f(t) \cdot s(t), \tag{98}$$

where $s(t)$ is the Fourier–transform of $P\frac{1}{\omega}$.
Show that $s(t) = -\frac{i}{2}\text{sign}(t)$ with sign(t) = +1 for $t > 0$ and sign(t) = −1 for $t < 0$.
Thus the Hilbert–transformation can be performed by two Fourier–transformations: First transform from ω to time–domain, multiply by $s(t)$ and transform back to frequeny domain. Numerically, this can be done efficiently by standard FFT routines [21].
Hint: Prove that the Fourier–transform of $s(t)$ is $P\frac{1}{\omega}$. Use an adiabatic switching–factor $exp(-\delta \mid t \mid),\ \delta \to 0^+$.

IV.B. Oscillator with a Quadratic Nonlinearity

We consider the case of charges bound in a noncentrosymmetric crystal which can be modelled by adding a quadratic force term in the Lorentz–model Eq.(19). (For simplicity spatial dispersion and vector properties of $\mathcal{P}$ and $\mathcal{E}$ will be omitted.)

$$\Big[\frac{d^2}{dt^2} + \gamma\frac{d}{dt} + \omega_0^2\Big]\mathcal{P}(t) + \lambda\mathcal{P}^2(t) = \epsilon_0\Omega_p^2\mathcal{E}(t). \tag{99}$$

No analytic solution of Eq.(99) is known, which is not surprising, as this model contains rich physics from periodic to chaotic phenomena. Note that there are two independent parameters λ and Ω_p^2 which can be used to set up perturbation expansions.
If $\mathcal{E}(t)$ is sufficiently weak, the nonlinear term $\lambda\mathcal{P}^2$ will be much smaller than the "restoring-force" $-\omega_0^2\mathcal{P}$ so that a pertubation expansion of $\mathcal{P}(t)$ of the form Eq.(17) may be used

$$\mathcal{P}(t) = \mathcal{P}^{(1)}(t) + \mathcal{P}^{(2)}(t) + \mathcal{P}^{(3)}(t)\ldots. \tag{100}$$

The various orders obey the following chain of differential equations

$$\Big[\frac{d^2}{dt^2} + \gamma\frac{d}{dt} + \omega_0^2\Big]\mathcal{P}^{(1)}(t) = \epsilon_0\Omega_p^2\mathcal{E}(t), \tag{101}$$

$$\Big[\frac{d^2}{dt^2} + \gamma\frac{d}{dt} + \omega_0^2\Big]\mathcal{P}^{(2)}(t) = -\lambda\left[\mathcal{P}^{(1)}(t)\right]^2, \tag{102}$$

$$\Big[\frac{d^2}{dt^2} + \gamma\frac{d}{dt} + \omega_0^2\Big]\mathcal{P}^{(3)}(t) = -2\lambda\Big[\mathcal{P}^{(1)}(t)\mathcal{P}^{(2)}(t)\Big]. \tag{103}$$

The first-order solution is identical with the Lorentz-solution

$$\mathcal{P}^{(1)}(\omega) = \epsilon_0\chi^{(1)}(\omega)\mathcal{E}(\omega), \tag{104}$$

$$\chi^{(1)}(\omega) = \Omega_p^2 G(\omega), \tag{105}$$

$$G(\omega) = \frac{1}{\omega_0^2 - \omega^2 - i\gamma\omega}. \tag{106}$$

In mathematics, $G(\omega)$ is termed (retarded) Green–function of Eq.(101).
The nonlinear susceptibilities are calculated in an analogous manner, where the products on the rhs of the equations for $\mathcal{P}^{(k)}(t)$ become convolutions in the frequency

domain, e.g.

$$G^{-1}(\omega)P^{(2)}(\omega) = -\lambda\int\frac{d\omega'}{2\pi}\mathcal{P}^{(1)}(\omega-\omega')\mathcal{P}^{(1)}(\omega'), \tag{107}$$

$$G^{-1}(\omega)\mathcal{P}^{(3)}(\omega) = -2\lambda\int\frac{d\omega'}{2\pi}\mathcal{P}^{(1)}(\omega-\omega')\mathcal{P}^{(2)}(\omega'). \tag{108}$$

Inserting Eq.(105) in Eqs.(107,108) the higher order susceptibilities can be read–off:

$$\chi^{(2)}(\omega_1,\omega_2) = -\lambda\Omega_p^4 G(\omega_1)G(\omega_1+\omega_2)G(\omega_2), \tag{109}$$

$$\chi^{(3)}(\omega_1,\omega_2,\omega_3) = -2\lambda^2\Omega_p^6 G(\omega_1)G(\omega_2)G(\omega_3)G(\omega_1+\omega_2+\omega_3) \times\frac{1}{3}\Big[G(\omega_1+\omega_2)+G(\omega_1+\omega_3)+G(\omega_2+\omega_3)\Big]. \tag{110}$$

Eq.(110) for the cubic susceptibility has second-order poles in the degenerate case (some of the ω_n are equal). The origin of these singularities is seen from the geometric expansion [7]

$$\frac{1}{x-a} = \frac{1}{x}+\frac{a}{x^2}+\frac{a^2}{x^3}\ldots, \quad |\,a\,|<|\,x\,|\,. \tag{111}$$

The *lhs* of Eq.(111) has a first-order pole at $x=a$, but the expansion on the *rhs* shows poles of all orders at $x=0$, yet the expansion is not valid there. In Eq. (110) the situation is of the same type. The remedy of the "dangerous" terms (poles of second and higher order) in Eq.(110) is a partial resummation of all singular terms in the infinite perturbation series (100). For a monochromatic field with frequency near ω_0 we have

$$P^{(1)}(t)+P^{(3)}(t)+\cdots=\epsilon_0\Big\{1+\frac{\lambda^2}{\omega_0^2-\omega^2-i\gamma\omega}|\chi^{(1)}\mathcal{E}|^2+\ldots\Big\}\chi^{(1)}(\omega)E(\omega). \tag{112}$$

The first terms of this expansion might be thought as the beginning of a geometric series. Summation can be cast in the quasilinear form:

$$P(t) = \epsilon_0\chi(\omega;E)E(\omega), \tag{113}$$

$$\chi(\omega;E) = \frac{\Omega_p^2}{\Omega^2-\omega^2-i\gamma\omega}, \qquad \Omega^2=\omega_0^2-\lambda^2\,|P|^2\,, \tag{114}$$

where Ω describes an intensity dependent eigenfrequency. For stationary fields, its quantum analogue is termed Stark–effect.

Problems:

10.) Calculate the amplitude–dependent eigenfrequency $\Omega=\Omega(A_1)$ of the nonlinear undamped oscillator

$$\frac{d^2x(t)}{dt^2}+x+\lambda x^2=0 \tag{115}$$

up to second order in the amplitude A_1 of the fundamental mode:

$$x(t)=\sum_{m=-\infty}^{\infty}A_m e^{im\Omega t}, \quad A_{-m}=A_m^*. \tag{116}$$

Hints: First, derive the set of nonlinear equations for A_m. Then, expand the equations for $m=0,1,2$ to leading order in A_1. Note that A_0, A_2 are proportional to the square of A_1, other coefficients A_m are of higher order.

IV.C. Photogalvanic Effect

According to the standard rules of irreversible thermodynamics a steady-state (non-supra) current in a solid is always driven by the gradient of the electrochemical potential $\eta = \mu + e\phi$ [22],

$$j = -\frac{\sigma}{e}\text{grad}\ \eta. \tag{117}$$

μ and ϕ denote the chemical and electrical potential of the charge carriers, respectively. Thus, inhomogeneities are necessarily needed which may either reside in the system itself (e.g. a $p-n$ junction) or are imposed by external conditions (e.g. gradients in temperature or electrical potential). In addition, a photo–induced current solely depends on the number of absorbed photons (regardless of their polarization) and the open circuit voltage is limited by the band gap of the semiconductor.
In noncentrosymmetric crystals, however, an additional direct current originates from the quadratic term in the current-field relation (46):

$$j_\alpha = IP_{\alpha\beta\gamma}(\omega)e_\beta e^*_\gamma. \tag{118}$$

In contrast to Eq.(117) this bulk photovoltaic current is intimately connected to the light polarization described by the complex polarization vector $\mathbf{e}$ and intensity I. $P_{\alpha\beta\gamma}(\omega) \sim \sigma^{(2)}_{\alpha\beta\gamma}(\omega, -\omega)$. Such a third rank tensor exists in all noncentrosymmetric crystals. In particular ferroelectrics, like $LiNb0_3$, allow for nonzero tensor elements with equal indices $\beta = \gamma$, and, hence, a photocurrent can occur even for unpolarized light. The phenomenon described by Eq.(118) in now called photogalvanic effect (PGE). For a survey and further references see Ruppel et al. [23] or v. Baltz [24].
For sake of completeness, we note that there is another contribution to the radiation impressed current which, in distinction to Eq.(118), explicitely depends on the direction of light propagation and, hence, is related to the momentum of the absorbed photons. This phenomenon is called photon drag effect but it is mainly important in the IR region.
There were many fingerprints of the PGE before Glass at Bell Laboratories [25] recognized it as a new photovoltaic mechanism whose spectacular property is the occurence of photovoltages larger than 100 kV even under perfect homogeneous conditions. Astonishingly, the main research activities were almost exclusively done later in the former Sovietunion so that this phenomenon is rarely known in the western hemisphere. To illustrate the discovery and some of its unusual properties of the PGE we give some examples.

- Local changes of indices of refraction were observed in ferroelectrics upon illumination. This leads to a (reversible) "damage" of the phase-matching conditions when using these materials in nonlinear optics. This photorefractive effect results from a small imposed current which charges the faces of the crystal. In a high resistive crystal, like $LiNbO_3$ the (intensity dependent) resistivity is in the range of $\rho \approx 10^{15} \ldots 10^{12} \Omega cm$ so that even a tiny current can lead to very large electric fields. According to the Pockels effect, this field causes a change in the refractive index, Fig. 8.

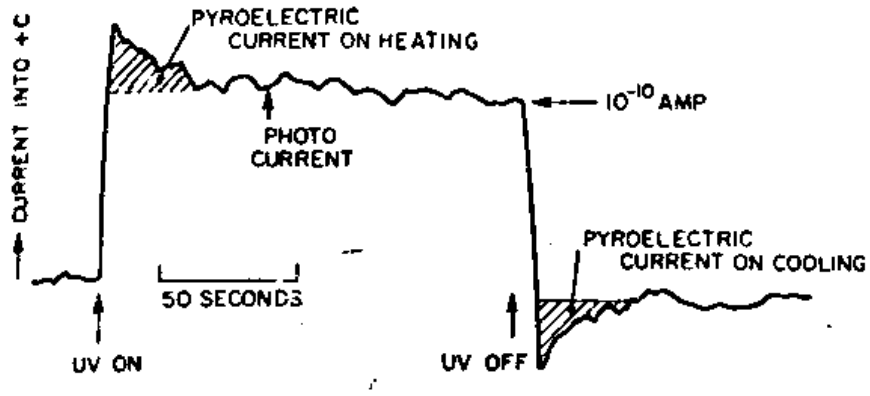

Fig. 8 *Current flow into the c faces of $LiNbO_3$ vs time with uv illumination. From Chen [26].*

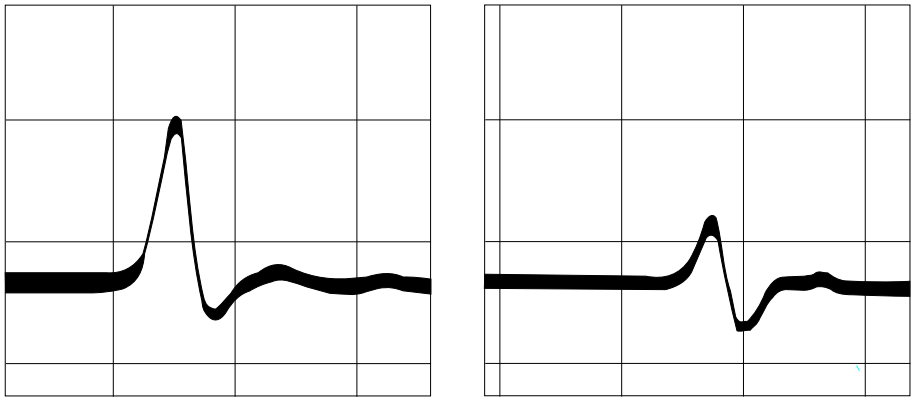

Fig. 9 *Oscilloscope traces of the optical rectification from $LiTaO_3$. (Left) Cu–doped, (right) undoped crystal. Time scale 2 nsec/div. From Auston et al. [27].*

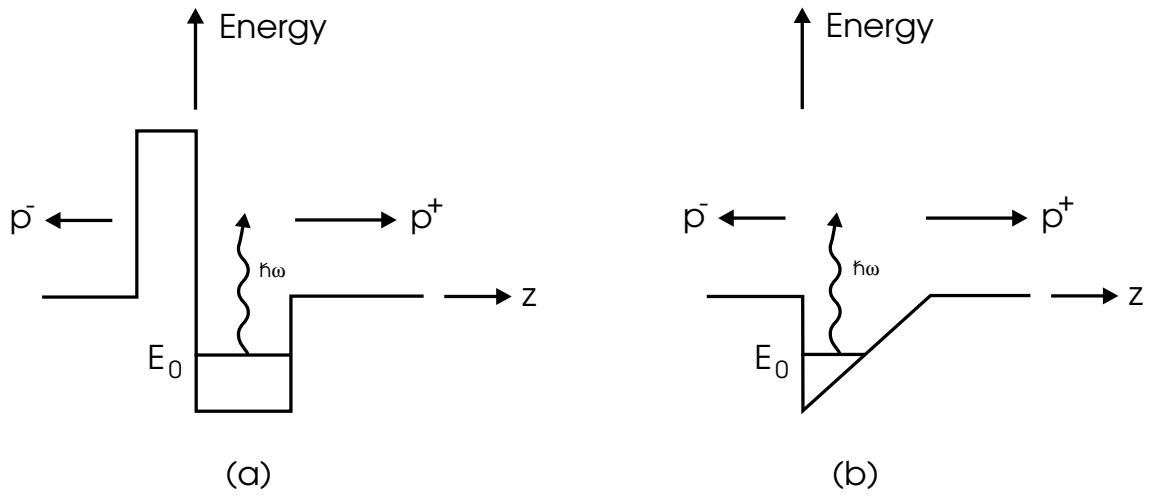

Fig. 10 *Optical transitions from impurities in a ferroelectric crystal resulting in a difference between the generation rates in $\pm z$ direction. Asymmetric potentials, (a) with and (b) without a barrier. From Ruppel et al. [23].*

- Austin et al. [27] discovered efficient "optical rectification" in polar crystals due to impurity absorption. The induced current contains two contributions: one from genuine OR following the derivative of the intensity profile of the laser and a photogalvanic current proportional to the light intensity, Fig. 9.

- Glass [25] recognized the PGE as originating from an asymmetry in the optical transition probabilities, Fig. 10. In a ferroelectric the transition probalitities p_+ and p_- from a bound $(Fe,\ Cu)$ impurity state to the conduction band can be different in $\pm c$ directions thus leading to a net charge transfer along the c–direction upon optical excitation. This asymmetry is not compensated under recombination because these processes are mostly nonradiative.

  It is convenient to represent the photogalvanic current in the following form:

$$j_{\rm PGE} = I\ \kappa\ K = e\ \frac{I}{\hbar\omega}\ K\ s, \quad s = (p_+ - p_-)\lambda, \tag{119}$$

  where K is the absorption constant, $\kappa = \frac{e}{\hbar\omega}s$ the Glass–constant, λ the mean free path of the photoexcited carriers, and s the anisotropy distance ("Schublänge"). For $LiNbO_3$ $s \approx 1A$ whereas for $KNbO_3$ $s \approx 18A$. Recent investigations of the photogalvanic tensor components of $LiNbO_3$ were reported by Karabekian and Odulov [28].

- The tensorial dependence of the photogalvanic current in n–doped GaP on the light polarization was studied by Gibson et al. [29] in connection with the investigation of fast responding IR detectors, Fig 11. GaP is a noncentrosymmetric cubic crystal with $\bar{4}3m$ point symmetry. Therefore, the only nonvanishing components of the photogalvanic tensor are $P_{123} = P_{132}$ and cyclic permutations of indices. Linear polarized light propagating along the z–direction induces a photogalvanic current which varies sinusoidally with the polarization of light

$$j_z = I\ P_{123}\ \sin 2\phi. \tag{120}$$

  ϕ is the angle between the polarization vector and the crystal x–axis.

- In GaP the microscopic mechanism of the PGE is different from the "ballistic" mechanism in $LiNbO_3$. The spectral shapes of the photogalvanic current and the interband optical absorption are almost identical which indicates that the PGE is due to transitions near the X point from the conduction band minimum to the next upper band. However, this apparently contradicts the bandstructure theory! According to time–reversal symmetry the band structure obeys $E(-\mathbf{k}) = E(\mathbf{k})$ so that the velocities $\mathbf{v}(\mathbf{k}) = \nabla E(\mathbf{k})$ at $\pm\mathbf{k}$ have opposite sign. As the transition rates are the same at $\pm\mathbf{k}$ there is no net current upon photoexcitation regardless of crystal symmetry. Most remarkably, however, there is a shift in real space of the valence and conduction band wave–packets upon photoexcitation, Fig. 12. In noncentrosymmetric crystals, these shift vectors at $\pm\mathbf{k}_0$ do not compensate each other and lead to a photogalvanic current which can be represented as [30]:

$$\begin{aligned}
\mathbf{j}_{\rm PGE} &= |e|\frac{I}{\hbar\omega}\frac{e^2}{2\pi^2\epsilon_0 m_0^2 nc\omega^2}\int (f_c - f_v)\,|< c\mathbf{k}\,|\mathbf{ep}|\,v\mathbf{k} >|^2 \times \\
&\quad \mathbf{s}(\mathbf{k})\ \delta(E_c(\mathbf{k}) - E_v(\mathbf{k}) - \hbar\omega)\ d^3k, && (121)\\
\mathbf{s}(\mathbf{k}) &= \mathbf{X}_{cc}(\mathbf{k}) - \mathbf{X}_{vv}(\mathbf{k}) + \nabla_{\mathbf{k}}\Phi_{cv}(\mathbf{k}), && (122)\\
\mathbf{X}_{mn}(\mathbf{k}) &= \int_{unitcell} i\ u^*_{m\mathbf{k}}(\mathbf{r})\nabla_{\mathbf{k}} u_{n\mathbf{k}}(\mathbf{r}) d^3r. && (123)
\end{aligned}$$

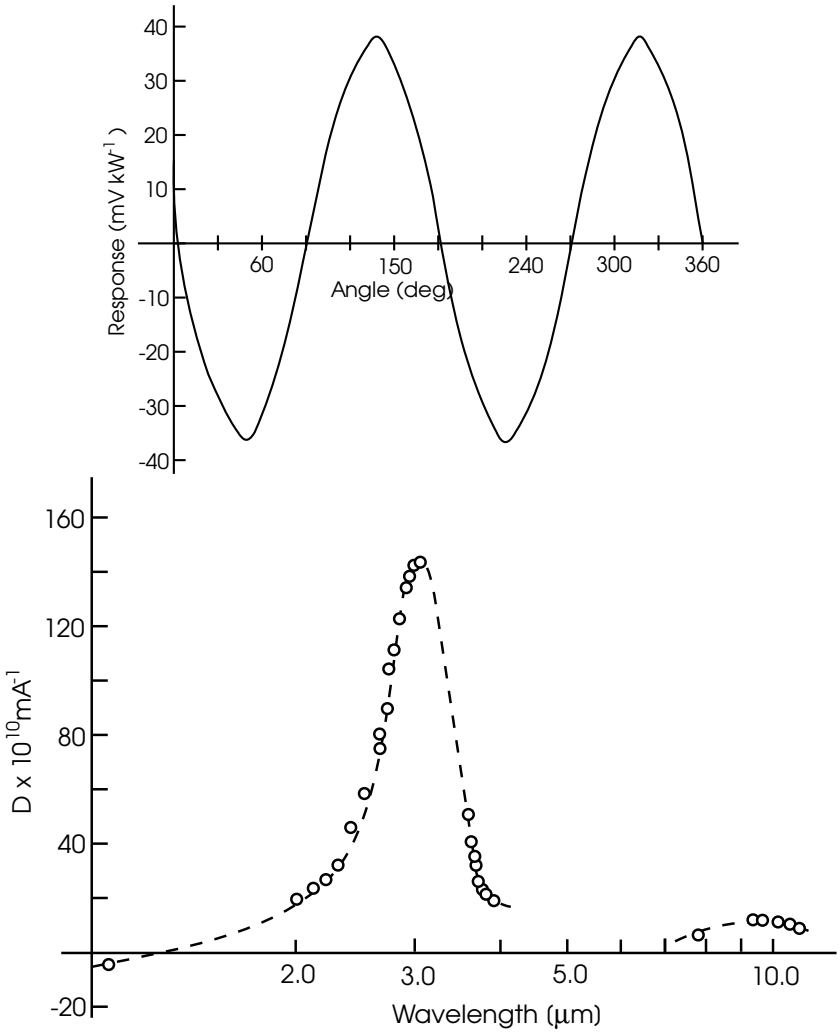

Fig. 11 *Photogalvanic effect in n–doped GaP. (Left) dependence on the light polarization, (right) spectral dependence,* $D = P_{123}/\sigma_{dc}$. *From Gibson et al. [29].*

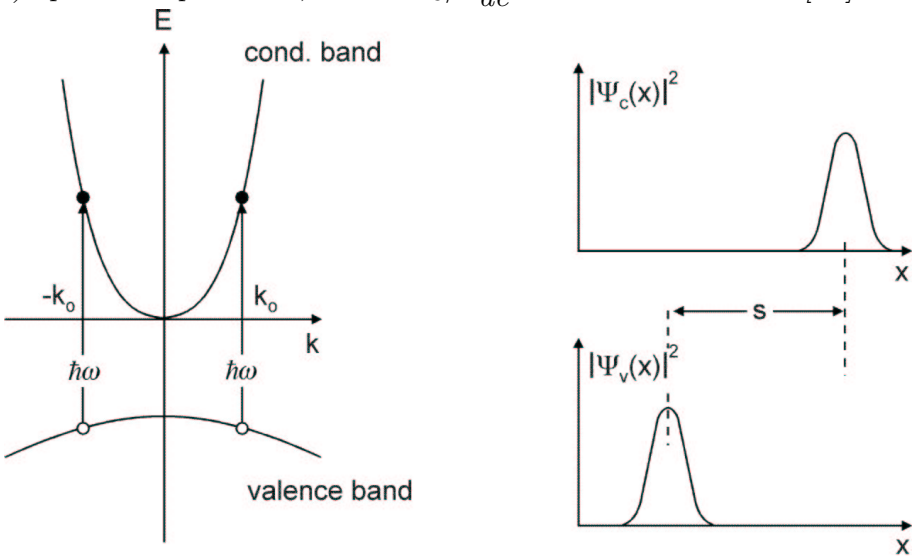

Fig. 12 *Optical transitions of wave packets in a noncentrosymmetric semiconductor. (Left)* **k***–space, (right) real space.*

$\Phi_{cv}(\mathbf{k})$ denotes the phase of the interband momentum matrix element $< c\mathbf{k}|\mathbf{ep}|v\mathbf{k} >$, n is the refractive index of the material, and $u_{n\mathbf{k}}(\mathbf{r})$ is the periodic part of the electron Bloch function. For the $X_1 \rightarrow X_3$ transition in GaP the shift of wave packets is $s \approx 8\AA$.

The shift vectors $\mathbf{X}_{mn}(\mathbf{k})$ are known for almost 40 years from the work of Adams and Blount [31] in connection with the Bloch–representation of the position operator. However, these quantities are rarely explicitely used or even notified. Exceptions are e.g. their connection to Bloch–oscillations, e.g. [32], nonlinear optical susceptibilities [33], or the definition macroscopic polarization in a ferroelectric or piezolectric materials in terms of a Berry–phase [34].
Recently the PGE and related phenomena found new interest. For example Schneider et al. [35] reported on IR photodetectors which were made of asymmetric quantum wells, directed motion of Brownian particles was proposed to occur in "thermal ratchets" (=periodic arrangement of potentials given in Fig. 10b) upon periodic perturbation [36],[37], or small amplitude swimming of a pulsating body [38]. The unifying aspect is the occurence of an unidirectional motion from oscillatory disturbances in noncentrosymmetric structures.

IV.D. Photon–Echo

The analogy of the TLS with the Spin-problem offers the description of an interesting phenomenon which is called photon–echo. Here, we examine the rather marvellous notion that not all decay processes are irreversible. This technique was developped by Hahn [39] for nuclear spin systems and, apart from its beautiful physics, it plays an important role to measure the T_2–time. For a survey and thorough discussion we refer to chapter 9 of Allen and Eberly [17].
In an experiment many TLS are involved and because of different local environments these have individually slightly different transition frequencies (=inhomogeneous line broadening, spectral width is parameterized by $1/T_2^*$). To describe the dynamics of the Bloch–vector it is convenient to transform to a frame rotating with the frequency of the light around the 3–axis:

$$R_1(t) = S_1(t)\cos\omega t - S_2(t)\sin\omega t, \tag{124}$$
$$R_2(t) = S_1(t)\sin\omega t + S_2(t)\cos\omega t, \tag{125}$$
$$R_3(t) = S_3(t). \tag{126}$$

(In complex notation the $1,2$ components are summarized by $R = Se^{i\omega t}$.) In this frame the equations of motion become [3]:

$$\dot{R}_1(t) = -\nu R_2(t) - \frac{R_1(t)}{T_2}, \tag{127}$$
$$\dot{R}_2(t) = +\nu R_1(t) + \omega_R R_3(t) - \frac{R_2(t)}{T_2}, \tag{128}$$
$$\dot{R}_3(t) = -\omega_R R_2(t) - \frac{R_3(t) - R_3^{eq}}{T_1}. \tag{129}$$

These linear differential equations have constant coefficients so that the solution can be found by an exponential Ansatz. In particular, for $\omega_R = 0$ the Bloch–vector performs

[3] Some signs are different from Allen and Eberly [17] who use a different numbering of the ground state and excited state.

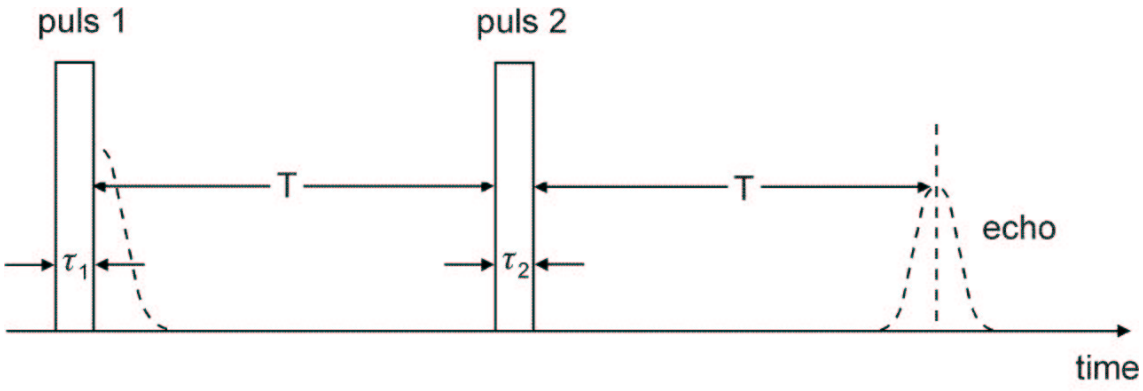

Fig. 13 *Pulse condition for the photon echo experiment. (Full lines) externally applied pulses, (dashed lines) polarization which give rise to the free polarization decay and the echo.*

a (damped) Larmor–precession around the 3–axis:

$$R_1(t) = [R_1(0)\cos\nu t - R_2(0)\sin\nu t]\; e^{-\frac{t}{T_2}}, \tag{130}$$

$$R_2(t) = [R_1(0)\sin\nu t + R_2(0)\cos\nu t]\; e^{-\frac{t}{T_2}}, \tag{131}$$

$$R_3(t) = R_3(0)\, e^{-\frac{t}{T_1}}. \tag{132}$$

At resonance, $\nu = 0$, and neglecting damping a light pulse causes a rotation of the Bloch–vector around the 1–axis:

$$R_1(t) = +R_1(0), \tag{133}$$

$$R_2(t) = +R_2(0)\cos\omega_R t + R_3(0)\sin\omega_R t, \tag{134}$$

$$R_3(t) = -R_2(0)\sin\omega_R t + R_3(0)\cos\omega_R t. \tag{135}$$

In the discussion of a photon–echo experiment four periods have to be distinguished, Fig. 13. To simplify matters, we shall assume that the pulse duration is short with respect to T_1, T_2, T_2^* and intense, $\omega_R T_2^* >> 1$, so that the influence of damping and detuning can be safely neglected during the pulses.

1. All TLS start from the same initial state $\mathbf{R}^{(0)} = (0,0,1)$. Then the ensemble of atoms is polarized by a first light pulse (duration τ_1) which leads to a common Bloch vector $\mathbf{R}^{(1)} = (u,v,w)$.

2. After the first light pulse the individual Bloch-vectors $\mathbf{R}^{(2)}$ precess according to Eqs.(130-132). Because of their slightly different frequencies the individual dipolemoments get out of phase and add to zero in a time T_2^* which is much shorter than T_2.

3. After time T a second light pulse is applied (duration τ_2, phase $\phi_2 = \omega_R\tau_2$) which according to Eqs.(133 - 134) "tips" the polarization to $\mathbf{R}^{(3)}$.

4. After the second pulse the Bloch–vectors $\mathbf{R}^{(4)}$ again rotate freely around the 3–axis. As a result, we obtain for the 1–component:

$$R_1^{(4)}(t) = \Big\{ u\,[\cos\nu T\cos\nu t - \cos\phi_2\sin\nu T\sin\nu t] \tag{136}$$

$$-v\,[\sin\nu T\cos\nu t + \cos\phi_2\cos\nu T\sin\nu t]\Big\}\, e^{-\frac{t+T}{T_2}} \tag{137}$$

$$+w\sin\phi_2\sin\nu t\; e^{-\frac{t+T}{T_1}}, \tag{138}$$

where the time t counts from the end of the second pulse. For $\phi_2 = \pi$ the terms in the [..] brackets combine to $\cos\nu(t-T)$ and $\sin\nu(t-T)$ and all individual Bloch–vectors again are in phase at time $2T$ after the first pulse, and add up in phase to a macroscopic polarization. This causes the emission of a light pulse, the photon echo.

The resurrected free polarization signal has the magic quality of something coming from nothing. However, this resurrection is only possible for times which are comparable with the T_2–time. For larger times, the intensity of the photon echo decays as the square of $\exp(-2T/T_2)$ i.e. $\exp(-4T/T_2)$. T_2 is also called dephasing–time.
It is interesting that the existance of the echo is not attributed to the π–character of the second pulse as it is frequently imputed. When decomposing the products of trigonometric functions $\cos\nu T\cos\nu t$ etc., in terms of sum and differences we realize that there is a contribution to the polarization of the form:

$$R_1^{(4)} = \frac{1-\cos\phi_2}{2}\Big\{u\cos\left[\nu(T-t)\right] - v\sin\left[\nu(T-t)\right]\Big\}e^{-\frac{t+T}{T_2}} + \ldots \tag{139}$$

Thus, a second pulse of any duration will induce an echo. However, its intensity is largest for $\phi_2 = \pi$.

Problems:

12.) Find the general solution of the coupled set of differential equations Eqs(127-129) for the Bloch–vector $\mathbf{R}(t)$. Express the integration constants in terms of $\mathbf{R}(0)$.
Hint: The solution can be obtained by an exponential Ansatz $\mathbf{R}(t) = \boldsymbol{\rho}\exp(\lambda t)$, where $\boldsymbol{\rho}$ is a time–independent 3–component vector.

IV.E. Linear Susceptibility: Excitons

To demonstrate the potential and simplicity of the SBE (e.g. compared with an evaluation of the Kubo formula) we derive the linear optical susceptibility of the interacting electron-hole system in the low excitation limit. This will lead us to the exciton and the famous Elliott–formula for the optical absorption.
At zero temperature $n_v = n_h = 0$ and the set of Eqs.(83-85) reduce to:

$$i\hbar\frac{\partial P(\mathbf{k},t)}{\partial t} = \Big[E_g + \frac{\hbar^2\mathbf{k}^2}{2m_r}\Big]P(\mathbf{k},t) - \frac{1}{V}\sum_{\mathbf{q}} V(\mathbf{k}-\mathbf{q})P(\mathbf{q},t) - p\mathcal{E}(t), \tag{140}$$

where m_r denotes the reduced electron-hole mass. In addition to the optical Bloch Eqs.(76-78) there is a interaction part which couples different $\mathbf{k}$'s so that $\mathbf{k}$ is no longer just a parameter. However, this interaction term is of convolution type and the integral equation can be Fourier-transformed to a well known differential equation:

$$i\hbar\frac{\partial P(\mathbf{r},t)}{\partial t} = \Big[E_g + \frac{\hbar^2}{2m_r}\Delta\Big]P(\mathbf{r},t) - V(\mathbf{r})P(\mathbf{r},t) - p\,\mathcal{E}(\mathbf{r},t)\,\delta(\mathbf{r}). \tag{141}$$

This is the (inhomogeneous) Schrödinger equation of the hydrogen atom, $\mathcal{P}(\mathbf{r},t)$ playing the part of the wave–function.
For $\mathcal{E}(\mathbf{r},t) = 0$ the stationary states are well known from standard texts on Quantum

Mechanics.

$$P_{\rm stat}(\mathbf{r},t) = \exp\Big(-i\frac{E_\mu}{\hbar}t\Big)\Psi_\mu(\mathbf{r}), \tag{142}$$

$$E_\mu = -\frac{Ry^*}{n^2}, \tag{143}$$

$$Ry^* = 13.56\frac{m_r/m_0}{\bar{\epsilon}^2}\ \text{eV}, \tag{144}$$

with the quantum numbers $\mu = (n, l, m)$, which have their usual meaning and run over the discrete as well as over the continuum states. In a semiconductor, the (bound) hydrogenic states are called excitons [3]. If the excitonic Rydberg Ry^* is smaller than the LO–phonon energy $\bar{\epsilon}$ is given by the static dielectric constant ϵ_s, otherwise $\bar{\epsilon} = \epsilon_\infty$. For $\mathcal{E}(\mathbf{r},t) \neq 0$ we seek the solution of $P(\mathbf{r},t)$ in terms of the complete set of the stationary states (142):

$$P(\mathbf{r},t) = \sum_\mu Q_\mu(t) e^{-i\frac{E_\mu}{\hbar}t}\Psi_\mu(\mathbf{r}). \tag{145}$$

$Q(\mathbf{r},t)$ can be found by a simple integration

$$Q_\mu(t) = ip\Psi_\mu(\mathbf{r}=0)\int_{-\infty}^{t}\mathcal{E}(t')e^{i\frac{E_\mu}{\hbar}t'}e^{\delta t}\,dt', \quad \delta\to 0^+, \tag{146}$$

from which it becomes obvious that only those excitonic states couple to the light which have nonvanishing wave function at the origin. These are the s–states. (This result, however, originates from our assumption $p_{cv}(\mathbf{k}) = const.$ If the dipole element becomes zero at the band edge the coupling is to p–states).
Inserting Eq.(145) in Eq.(80) and using the completeness relation of the stationary states Eq.(142),

$$\sum_\mu \Psi^*_\mu(\mathbf{r}')\Psi_\mu(\mathbf{r}) = \delta(\mathbf{r}-\mathbf{r}'), \tag{147}$$

we finally obtain the electron-hole-pair susceptibility as [14]

$$\chi(\omega) = 2|p_{cv}|^2\sum_\mu |\Psi_\mu(\mathbf{r}=0)|^2\left[\frac{1}{\hbar(\omega+i\delta+E_g+E_\mu)} - \frac{1}{\hbar(\omega+i\delta-E_g-E_\mu)}\right]. \tag{148}$$

Using the Dirac identity (97) the imaginary part is given by:

$$\chi_2(\omega) \propto \sum_{n=1}^{\infty}\frac{4\pi}{n^3}\delta(\Delta+\frac{1}{n^2}) + \theta(\Delta)\frac{\pi e^{\frac{\pi}{\sqrt{\Delta}}}}{\sinh(\frac{\pi}{\sqrt{\Delta}})}. \tag{149}$$

$\Delta = (\hbar\omega - E_g)/Ry^*$ denotes the normalized photon energy. This result is first derived by Elliott [40]. The corresponding real part can be calculated from the Kramers–Kronig relation (92). Recently Tanguy [41] succeeded to express the real part of the susceptibility in terms of known functions.
The optical absorption spectrum of a semiconductor is diplayed in Fig. 14 which gives a lively impression about the importance of the Coulomb interaction and excitonic states near the band gap. The optical absorption spectrum consists of a series with rapidly decreasing oscillator strength $\propto n^{-3}$ and a continuum part. In the very best samples excitonic lines up to $n = 3$ can be resolved, see [3] page 201. Close to the ionization continuum, $\Delta \to 0$ the absorption assumes a constant value, in striking difference with the square–root law for noninteracting bands. Thus, the attractive Coulomb interaction not only creates bound states below the gap but leads to a pronounced enhancement of the absorption above the gap. ("Sommerfeld–enhancement").

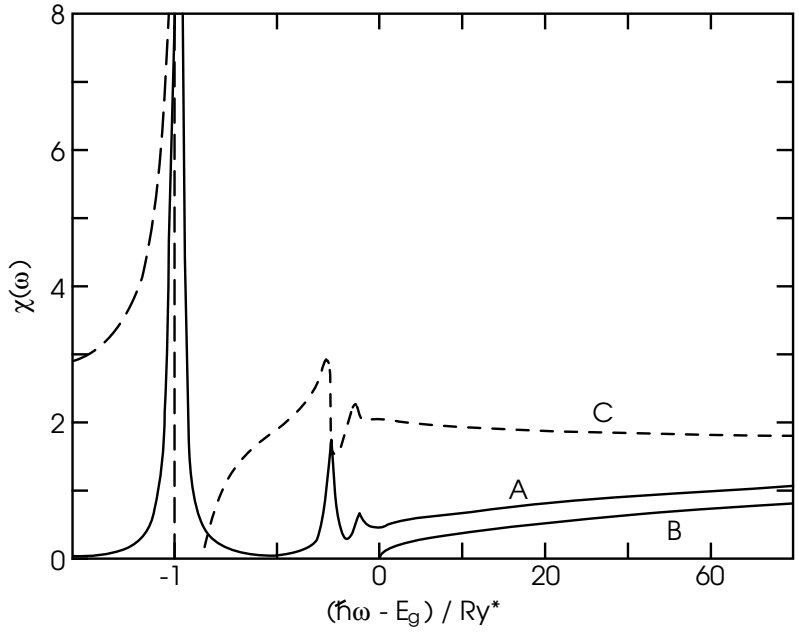

Fig. 14 *Susceptibility of a semiconductor near the gap energy: (A)* Im χ*, (C)* Re χ *of the interacting electron hole system, Eq.(149), (B)* Im χ *of the noninteracting system, Eq.(82). Note the different frequency scale above and below the gap. An appropriate broadening is included. From Stahl and Balslev [11].*

V. OUTLOOK

Sofar the damping mechanismn in the SBE was described phenomenologically. In a next step this can be improved by setting up kinetic (Boltzmann) equations for the electron and hole populations with appropriate collision integrals for the carrier–phonon scattering. These equations are coupled nonlinear differential–integral equations which can be solved only by advanced numerical treatments.
The many body effects which are omitted in the SBE as given by Eqs.(83- 85) lead to a further renormalization of the electronic energies, screening of the interactions, and additional collision terms. The success of this theory to descibe numerous linear and nonlinear effects is obvious from Haug and Koch [14] and the contributions presented by Klingshirn [42] and Hvam [43] in this book.
Recent studies by Stahl [44] and his collaborators indicate, however, that the SBE treatment becomes questionable for the tera–Hertz emission in a narrow band superlattice. For ulrashort pulses the formulation of collision integrals in terms of energy conserving processes is no longer possible and quantum kinetic equations are needed.

ACKNOWLEDGEMENTS

I thank Professor B. Di Bartolo for inviting me to Erice which, again, provided a stimulating summer school in a delightful atmosphere.
I also thank Mrs. R. Schrempp, Mrs. M. Bielfeld, Dr. Ch. Fuchs, and Dipl. Phys. A. Mildenberger for their help with the preparation of the article.

REFERENCES

1. L. D. Landau and E. M. Lifschitz, *Electrodynamics of Continuous Media*, Pergamon Press (1984).
2. F. C. Wooten, *Optical Properties of Solids*, Academic Press (1972).
3. C.F. Klingshirn, *Semiconductor Optics*, Springer (1995).
4. *Spectroscopy and Dynamics of Collective Excitations in Solids*, edited by B. Di Bartolo, NATO ASI Series B: Physics Vol. 356, Plenum Press (1997).
5. *Ultrafast Dynamics of Quantum Systems: Physical Processes and Spectroscopic Techniques*, edited by B. Di Bartolo, Plenum Press (This book).
6. L.V. Keldysh, D.A. Kirshnitz, and A.A. Maradudin eds., *The Dielectric Function of Condensed Systems*, North Holland (1989).
7. Yu. Il'inskij and L.V.Keldysh, *Electromagnetic Response of Material Media*, Plenum Press (1994).
8. P. Grosse, *Propagation of Electromagnetic Waves and Magnetooptics*, in *Theoretical Aspects and Developments in Magneto Optics*, edited by J. Devreese, Plenum Press (1980).
9. F. Forstmann and R.R. Gerhards, *Metal Optics Near the Plasma Frequency*, Springer Tracts in Modern Physics, Vol. 109, Springer (1986).
10. R. von Baltz, *Plasmons and Surface Plasmons in Bulk Metals, Metallic Clusters, and Metallic Heterostructures*, in [4].
11. A. Stahl and I. Balslev, *Electrodynamics of the Semiconductor Band Edge*, Springer Tracts in Modern Physics, Vol.110, Springer (1987).
12. B. Di Bartolo, *Propagation of waves in linear and nonlinear media*, in [5].
13. R.W. Boyd, Nonlinear Optics, Academic Press (1992).
14. H. Haug and S.W. Koch, *Quantum Theory of the Optical and Electronic Processes of Semiconductors*, World Scientific (1994).
15. R. Zimmermann, *Theoretical Description of Collective Excitations: Bloch equations and Relaxation Mechanisms*, in [4].
16. R.P. Feynman, R.B. Leighton, and M. Sands, *The Feynman Lectures on Physics*, Addison–Wesley (1966).
17. L. Allen and J.H.Eberly, *Optical Resonance and Two–Level Atoms*, Wiley (1975).
18. H.M. Nussenzweig, *Causality and Dispersion Relations*, Academic Press (1972).
19. W. Stößel, *Fourier Optik. Eine Einführung*, Springer (1993).
20. P.C. Martin, Phys. Rev. **161**, 143 (1967).
21. W.H. Press, B.P. Flannery, S.A. Teukolsky, and W.T. Vetterly, *Numerical Recipes*, Cambridge University Press (1986).
22. S.R. De Groot and P. Mazur, Non–Equilibrium Thermodynamics, North Holland (1962).
23. W. Ruppel, R. von Baltz, and P. Würfel, Ferroelectrics **43**, 109 (1981).
24. R. von Baltz, Ferroelectrics, **35**, 131 (1981).
25. A.M. Glass, D. von der Linde, and T.J. Negran, Appl. Phys. Lett. **25**, 233 (1974).

26. F.S. Chen, Jour. Appl. Phys. **40**, 3389 (1969).

27. D.H.Auston, A.M. Glass, and A.A. Ballman, Phys. Rev. Lett. **28**, 897 (1972).

28. S.I. Karabekian and S.G. Odulov, phys. stat. sol. (b) **169**, 529 (1992).

29. A.F. Gibson, C.B. Hatch, M.F. Kimmitt, S. Kothari, and S. Serafetinidis, J. Phys. **C10**, 905 (1977).

30. D. Hornung, R.von Baltz, and U. Rössler, Sol. State Comm. **48**, 225 (1983).

31. E.I. Blount, in *Solid State Physics*, edited by F. Seitz and D. Turnbull, Academic Press (1962), Vol 13.

32. C.F. Hart and D. Emin, Phys. Rev. **B43**, 4521 (1991) and references cited therein.

33. C. Aversa and J.E. Sipe, Phys. Rev. **B52**, 14 636 (1995).

34. R. Resta, Rev. Mod. Phys. **66**, 899 (1994).

35. H. Schneider et al. Superlattices and Microstructures, **20**, 1 (1996).

36. L.P. Faucheux, L.S. Bourdieu, P.D. Kaplan, and A.J. Libchaber, Phys. Rev. Lett. **74**, 1504 (1995).

37. P. Reimann, M. Grifoni, and P. Hänggi, Phys. Rev. Lett. **79**, 10 (1997).

38. B.U. Felderhof and R.B. Jones Physica, **A202**, 119 (1994).

39. E.L. Hahn, Phys. Rev. **80**, 580 (1950).

40. R.J. Elliott, in *Polarons and Excitons*, edited by C.G. Kuper and G.D. Whitfield, Oliver and Boyd (1969).

41. Ch. Tanguy, Phys. Rev. Lett. **75**, 22 (1995).

42. C. Klingshirn, *Ultrafast Spectroscopy of Semiconductors*, in [5].

43. J. Hvam, *Spectroscopy of Coherent Interactions between Light and Matter*, in [5].

44. V.M. Axt, G. Bartels, and A. Stahl, Phys. Rev. Lett. **76**, 2543 (1996).

SOLUTIONS

1a) The general solution of the first order differential equation for the current Eq.(18) consists of the general solution of the homogeneous equation, which is $C\exp(-\gamma t)$, and a particular solution of the inhomogeneous equation. The boundary condition requires that $C = 0$. The particular solution can be found by "variation of the constant", $C \to C(t)$ and yields:

$$\sigma(t-t') = \frac{ne^2}{m} e^{-\gamma(t-t')}\theta(t-t') \tag{150}$$

1b) The susceptibility in the time domain is the Green–function of Eq.(19), i.e. the particular solution for a delta–pulse $\mathcal{E}(t) = \delta(t-t')$ at fixed time t'. For $t < t'$, $\mathcal{P}(t) \equiv 0$, whereas for $t > t'$ the puls creates a free oscillation which rises continously from zero with slope $\epsilon_0\Omega_p^2$ so that the second derivative becomes a delta function. As a result, we obtain:

$$\chi(t-t') = \frac{\Omega_p^2}{\Omega_0}\, e^{-\frac{\gamma}{2}(t-t')} \sin\big[\Omega_0(t-t')\big]\theta(t-t'). \tag{151}$$

$\Omega_0^2 = \omega_0^2 - (\gamma/2)^2$. This result holds also for the overdamped and even for the critically damped case, $\omega_0 = \gamma/2$, if the appropriate limit is taken.

2.) In the homogeneous case the negative electron charge density compensates the positive ionic background charge so that $\mathcal{E} = 0$ everywhere. The presence of an external charge Q at $\mathbf{r} = 0$ attracts or repells the mobile electrons and, hence, induces an electrical field $\mathcal{E} = -\text{grad}\,\Phi$. In linear approximation, we obtain from Eq. (18):

$$\beta\,\text{grad}\,\rho(\mathbf{r}) = -\frac{e}{m^*}\,\rho_0\,\text{grad}\,\Phi(\mathbf{r}). \tag{152}$$

The required solution which fulfills the boundary condition $\Phi(\infty) = 0$, $\rho(\infty) = \rho_0$ is

$$\rho(\mathbf{r}) = -\frac{n_0 e}{m^*\beta}\,\Phi(\mathbf{r}) + \rho_0. \tag{153}$$

From the Poisson–equation

$$\Delta\Phi = -\frac{1}{\epsilon_0}\Big[Q\,\delta(\mathbf{r}) + \rho(\mathbf{r}) - \rho_0\Big], \tag{154}$$

we obtain the Thomas–Fermi equation for the potential

$$\Delta\Phi(\mathbf{r}) + \kappa^2\Phi(\mathbf{r}) = -\frac{1}{\epsilon_0}Q\,\delta(\mathbf{r}), \quad \kappa^2 = \frac{n_0 e^2}{\epsilon_0\beta m^*}. \tag{155}$$

The solution of Eq.(155) reads:

$$\Phi(\mathbf{r}) = \frac{Q}{4\pi\epsilon_0}\frac{1}{r}e^{-\kappa r}, \tag{156}$$

where $1/\kappa$ is the Thomas–Fermi screening length.

3.) Fourier–transformation of Eqs.(18,12) yield (in linear approximation)

$$(-i\omega + \gamma)\,\mathbf{j}(\mathbf{q},\omega) + \beta(-i\mathbf{q})\rho(\mathbf{q},\omega) = \frac{n_0 e^2}{m^*}\mathcal{E}(\mathbf{q},\omega), \tag{157}$$

$$-i\omega\rho(\mathbf{q},\omega) + \mathbf{q}\,\mathbf{j}(\mathbf{q},\omega) = 0. \tag{158}$$

For transverse fields $\mathbf{q}\,\mathbf{j} = 0$ so that $\rho = 0$ whereas in the longitudinal case $\rho = qj/\omega$. As a result we obtain:

$$\sigma_t(\mathbf{q},\omega) = \frac{\frac{e^2 n_0}{m^*}}{\gamma - i\omega}, \quad \sigma_\ell(\mathbf{q},\omega) = \frac{\frac{e^2 n_0}{m^*}}{\gamma - i(\omega - q^2/\omega)}. \tag{159}$$

Equivalently, we may describe $\mathbf{j}(\mathbf{r},t)$ as a displacement current with susceptibility $\chi = i\sigma/\omega\epsilon_0$ and dielectric function $\epsilon = 1 + \chi$ by

$$\epsilon_\ell(\mathbf{q},\omega) = 1 - \frac{\omega_p^2}{\omega(\omega + i\gamma) - \beta q^2}, \qquad \epsilon_t(\mathbf{q},\omega) = 1 - \frac{\omega_p^2}{\omega(\omega + i\gamma)}. \tag{160}$$

Neglecting damping, the dispersion of the longitudinal collective excitations (plasmons) $\omega = \omega(\mathbf{q})$ is determined by $\epsilon(\mathbf{q},\omega) = 0$:

$$\omega(\mathbf{q}) = \sqrt{\omega_p^2 + \beta\mathbf{q}^2} \tag{161}$$

4) Fourier–transformation of Eq.(19) together with $\mathcal{P} = \epsilon_0\chi\mathcal{E}$ yields:

$$\chi_\ell(\mathbf{q},\omega) = \frac{\Omega_p^2}{\omega_0^2 - \omega^2 - i\gamma\omega - \beta q^2}. \tag{162}$$

The dispersion of the transverse collective excitations in given by the poles of $\chi_\ell(\mathbf{q},\omega)$. As a result we have in the limit of small wave–numbers

$$\omega(\mathbf{q}) = -\frac{i\gamma}{2} + \omega_0 + \frac{\beta}{2\omega_0}q^2. \tag{163}$$

This result agrees qualitavely with the dispersion of TO phonons near $\mathbf{q} = 0$ [3].

5.) Off resonance the solution of Eqs.(63-64) reads:

$$d_1(t) = \left[\cos\left(\frac{\Omega_R}{2}t\right) - i\frac{\nu}{\Omega_R}\sin\left(\frac{\Omega_R}{2}t\right)\right] e^{i\frac{\nu}{2}t}, \tag{164}$$

$$d_2(t) = i\frac{\omega_R}{\Omega_R}\sin\left(\frac{\Omega_R}{2}t\right) e^{-i\frac{\nu}{2}t}. \tag{165}$$

The probability finding the atom in the excited state is

$$\mid d_2(t) \mid^2 = \left(\frac{\omega_R}{\Omega_R}\right)^2 \sin^2\left(\frac{\Omega_R}{2}t\right). \tag{166}$$

For $\nu = \omega_R$ the Rabi–amplitude is reduced to $\frac{1}{2}$ and the period is shortened by a factor of $\frac{1}{\sqrt{2}}$ if compared with the resonant case.

6.) At resonance, there are two orthogonal states with $|d_j(t)|^2 = \text{const}$. These are obtained by chosing $a = \pm ib$ in Eqs.(63, 64):

$$d_+(t) = \frac{1}{\sqrt{2}}\begin{pmatrix} +1 \\ -1 \end{pmatrix} e^{-i\frac{\omega_R}{2}t}, \qquad d_-(t) = \frac{1}{\sqrt{2}}\begin{pmatrix} +1 \\ +1 \end{pmatrix} e^{+i\frac{\omega_R}{2}t}. \tag{167}$$

The state of the atom is represented by

$$\mid \Psi_+(t) = \frac{1}{\sqrt{2}}\left\{e^{-i(\epsilon_1+\frac{\omega_R}{2})t} \mid 1> - e^{-i(\epsilon_2+\frac{\omega_R}{2})t} \mid 2>\right\}, \tag{168}$$

$$\mid \Psi_-(t) = \frac{1}{\sqrt{2}}\left\{e^{-i(\epsilon_1-\frac{\omega_R}{2})t} \mid 1> + e^{-i(\epsilon_2-\frac{\omega_R}{2})t} \mid 2>\right\}. \tag{169}$$

These time–dependent states are the analoga of the stationary states $\mid 1>, \mid 2>$ of the isolated atom where the energies are replaced by $\epsilon_1 \pm \frac{\omega_R}{2}$, $\epsilon_2 \pm \frac{\omega_R}{2}$. Hence, an additional weak perturbing field with variable frequency will induce transitions at three different frequencies ω_0, $\omega_0 + \omega_R$, and $\omega_0 - \omega_R$, where $\omega_0 = (\epsilon_2 - \epsilon_1)/\hbar$. To observe the Rabi–splitting the amplitude of the driving field at frequency ω_0 has to be large enough so that ω_R is larger than the line width.

7.) The singularities of the response functions are located at:
a) Drude–conductivity: $\omega = -i\gamma$.
b) Drude–susceptibility: $\omega = 0$ and $-i\gamma$.
c) Lorentz–susceptibility: $\omega = -i\frac{\gamma}{2} \pm \sqrt{\omega_0^2 - \left(\frac{\gamma}{2}\right)^2}$
In the weak damping case there are two poles which lie closely below the real axis near the frequency of the undamped oscillator. With increasing damping these poles move towards the negative imaginary ω–axis. At critical damping there is a single quadratic pole at $\omega = -i\frac{\gamma}{2}$.

8.) Hilbert–transform of a box–function:
If $\omega \notin [-1, 1]$ the integral is not singular and it can be obtained by elementary means

$$g(\omega) = \frac{1}{\pi}\ln\left|\frac{1-\omega}{1+\omega}\right|. \tag{170}$$

For $\omega \in (-1,1)$ logarithmic terms $\ln\delta$ appear but, eventually, they drop out and the result given above even holds in this case. Note, the Hilbert–transform of the box function is antisymmetric and has logarithmic singularities at the edges of the box at $\omega = \pm 1$. For $\omega \to \infty$, $g(\omega)$ converges to zero as const/ω.

9.) Kramers–Kronig transformation by double Fourier–transformation.
When using Eq.(95) it is easy to verify that the Fourier–transform of $s(t)$ is $P\frac{1}{\omega}$.

10.) Anharmonic oscillator.
The coupled set of equations for the Fourier–coefficients read:

$$\left[1 - k^2\Omega^2\right] A_k + \lambda \sum_{m=-\infty}^{\infty} A_m A_{k-m} = 0. \tag{171}$$

In particular, the equations for $k = 0, 2$ are given by

$$\begin{aligned} A_0 + \lambda \left[2|A_1|^2 + O(A_1^4)\right] &= 0, & (172)\\ \left[1 - 4\Omega^2\right] A_2 + \lambda \left[A_1^2 + O(A_1^4)\right] &= 0. & (173) \end{aligned}$$

Up to second order in A_1 we obtain:

$$A_0 = -2\lambda|A_1|^2, \quad A_2 = \frac{\lambda}{3} A_1^2. \tag{174}$$

Inserting these results in Eq.(171) with $k = 1$:

$$\left[1 - \Omega^2\right] A_1 + \lambda \left[2A_0 A_1 + 2A_{-1}A_2 + O(A_1^5)\right] = 0 \tag{175}$$

yields up to second order

$$\Omega^2 - 1 = -\frac{10}{3}\lambda^2 |A_1|^2 \tag{176}$$

11.) The general solution of the Bloch Eqs.(127-129) (neglecting damping) are:

$$R_1(t) = R_1(0)\frac{\omega_R^2 + \nu^2 \cos\Omega_R t}{\Omega_R^2} - R_2(0)\frac{\nu}{\Omega_R}\sin\Omega_R t - R_3(0)\frac{\nu\omega_R}{\Omega_R^2}\left[1 - \cos\Omega_R t\right], \tag{177}$$

$$R_2(t) = +R_1(0)\frac{\nu}{\Omega_R}\sin\Omega_R t + R_2(0)\cos\Omega_R t + R_3(0)\frac{\omega_R}{\Omega_R}\sin\Omega_R t, \tag{178}$$

$$R_3(t) = -R_1(0)\frac{\nu\omega_R}{\Omega_R^2}\left[1 - \cos\Omega_R t\right] - R_2(0)\frac{\omega_R}{\Omega_R}\sin\Omega_R t + R_3(0)\frac{\nu^2 + \omega_R^2\cos\Omega_R t}{\Omega_R^2}. \tag{179}$$

In particular, on resonance $\nu = 0$ and for $\mathbf{R}(0) = (0, 0, 1)$ we obtain:

$$R_1(t) = 0, \quad R_2(t) = \sin\omega t, \quad R_3(t) = \cos\omega t. \tag{180}$$

Compare with Eq.(75) and Eqs.(124-125)!